AMIRA INTERNATIONAL

Progress Report

Confidential

P544 – Proterozoic sediment-hosted copper deposits

June 2002

Centre for Ore Deposit Research, University of Tasmania
Colorado School of Mines

AMIRA International Limited ACN 004 448 266 ABN 60 176 687 975
9th Floor 128 Exhibition Street Melbourne 3000 Australia Phone: +61 3 9679 9999 Facsimile: +61 3 9679 9900
email: AMIRA@amira.com.au Website www.amira.com.au

UNIVERSITY
OF TASMANIA

Produced by the
Centre for Ore Deposit Research
University of Tasmania
GPO Box 252-79,
Hobart Tasmania Australia 7001

June 2002

another Pongratz Production 2002

AMIRA International Limited
ACN 004 448 266 ABN 60 176 687 975
www.amira.com.au

CODES/CSM:AMIRA P544

Proterozoic Sediment-Hosted Copper Deposits

June 2002

Confidential to Sponsors

Contents

Introduction

This report contains two contributions from David Broughton that were to be presented at the P544 sponsors' meeting held in Adelaide in May 2002. The first report documents the transition from Lower Roan sediments to basement rocks in drill cores from Konkola East (Kawiri area) and Ndola East. The second report is a drill core-based detailed petrographic description of the mineralised sequence at Konkola with stratigraphically equivalent rocks from the barren gap and a fringe ore position.

Due to circumstances beyond his control David was unable to attend the meeting, and Robert Scott presented a synopsis of his findings on his behalf.

This report supersedes the meeting presentations.

Peter McGoldrick
June 2002

Petrology of Lower Roan–basement contacts, Konkola East and Ndola East areas

David Broughton
Colorado School of Mines

Summary

This report describes the Lower Roan–basement transition in two drill cores: one (KW26) from east of Konkola where Lower Roan sediments are in contact with Muliashi Porphyry, and the other (IT28) from near Ndola where Lower Roan is in contact with quartzo-feldspathic gneiss. In both holes the contacts are interpreted as unconformities with preserved (albeit metamorphosed) regoliths. In KW26 the transition is characterised by intense biotite-epidote alteration of feldspars, and in IT28 the transition is marked by high-angle fractures filled with sediment from the overlying sandstone. Lower Ron rocks in both locations show similar early diagenetic features such as oxide and clay coatings on detrital grains.

Introduction

This report describes samples of two drill cores selected to examine the nature of the basement–Katangan relationships, from holes drilled east of the Konkola mine and in the Ndola East area (Figure 1). The nature of the basement contact has been contentious since the earliest geological investigations in the Copperbelt, and remains poorly documented. The Copperbelt is underlain by basement of middle to late Proterozoic age, which consists predominantly of granites, schists/gneisses and quartzites. Of interest are the granites, most of which are of Ubendian age (1800 to 2000 Ma), and are locally termed the "old" or "grey" granites. Also present are "red" granites, including the Nchanga Red Granite, dated at 880 Ma, the youngest basement age obtained in the Copperbelt. The samples from hole KW26 in the Konkola East (Kawiri) area come from the Muliashi Porphyry, which has some petrological similarities to the Nchanga granite but has not been dated. Basement in the Ndola East hole IT28 consists of quartz-feldspathic gneiss of uncertain age.

This study used petrographic, cathodoluminescence and SEM studies of nine thin sections to document the original mineralogy and diagenetic/metamorphic/hydrothermal overprints of the basement and cover rocks, in order to place constraints on provenance, timing of diagenetic and hydrothermal events.

In both cores a zone of residual, weathered – but now metamorphosed – basement is interpreted to occur at the contact. In hole KW26, approximately 2.5 metres of residual Muliashi Porphyry is preserved, at a down-hole depth of 536.0 to 538.5 metres (thin sections 82, 83). In hole IT28, the depth of preserved basement weathering is at least 3 metres.

Konkola East (Kawiri) Area, Drill Hole KW26

Basement-Muliashi Porphyry (thin section 81)

The Muliashi porphyry forms the basement in the Konkola area, and is overlain by sandstones and conglomerates of the basal Lower Roan. There is considerable vertical relief on the basement

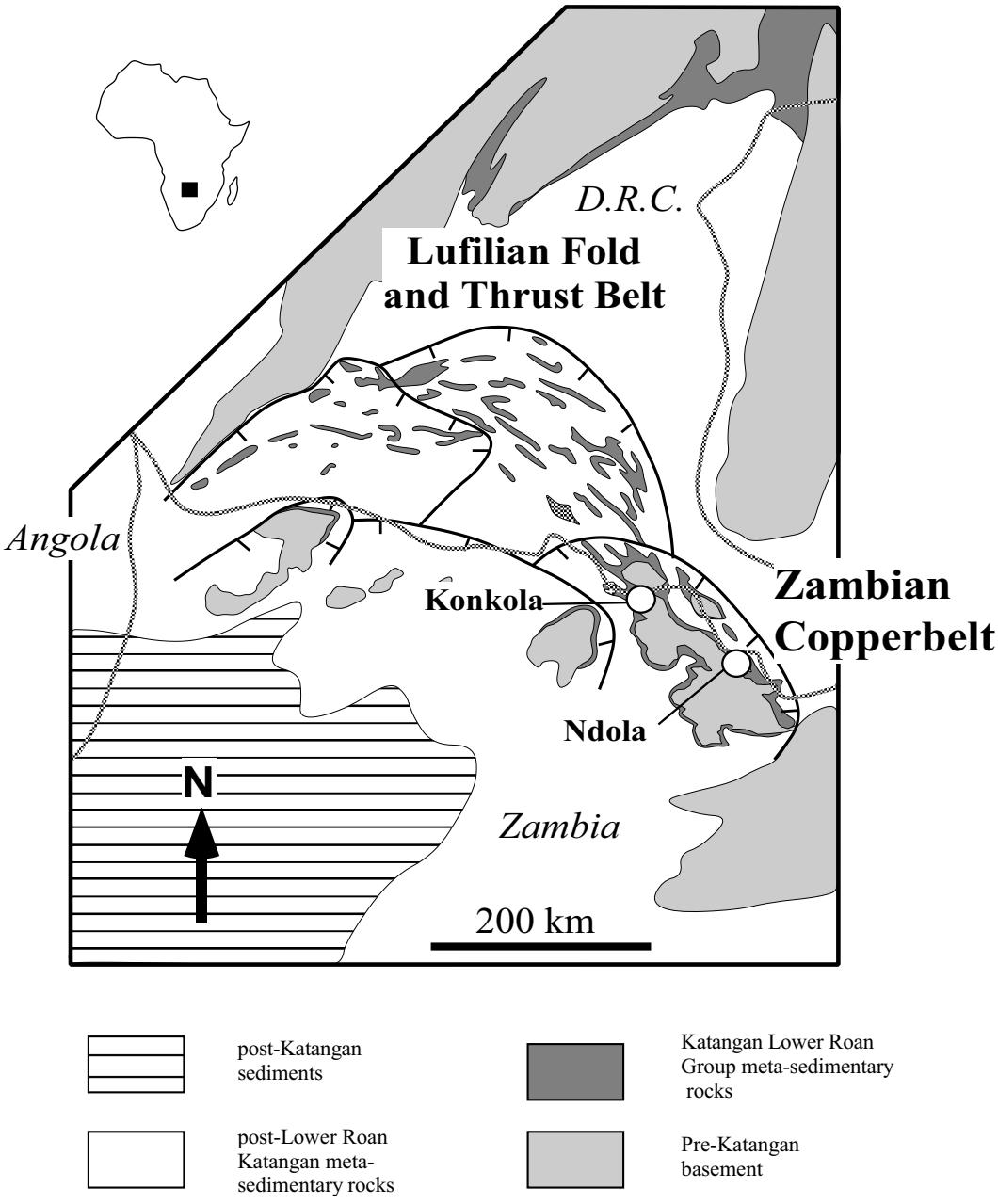

Figure 1. Location of Konkola mine (drill hole KW26) and Ndola property (drill hole IT28) within the Zambian Copperbelt.

topography: east of Konkola on the Kawiri (KW) property the Ore Shale is interpreted as missing (not deposited) against a local basement high, whereas in the area between Konkola and Musoshi a basal Lower Roan thicknesses of at least a kilometre are known from drilling.

In hand specimen, the Muliashi Porphyry consists of about 40% cm-sized pink phenocrysts of k-feldspar with conspicuous pale greenish sericitized plagioclase rims, in a groundmass of mm- to cm-sized bluish quartz (25%), greenish sericitized plagioclase (25%), and dark biotite (10%) (Figure 2). The phenocryst morphology is similar to a Rapakivi texture. Accessory sphene and magnetite can also be seen.

In thin section, the phenocrysts are seen to consist of perthitic microcline and orthoclase overgrown by plagioclase (Fig 3a, b). The k-feldspar typically forms multiple, optically continuous crystals that together comprise the phenocryst, separated by thin zones of interstitial quartz. The plagioclase is zoned, with epidote-biotite-(clinozoisite, calcite) altered cores and clear, unaltered rims. SEM/EDS examination confirms that the plagioclase cores are sodic-calcic, whereas the rims are sodic (albite). Under CL the k-feldspar is characteristically bluish, and the unaltered plagioclase and perthitic intergrowths brownish. The calcite has a red to golden yellow luminescence, indicating probable Fe and Mn substitution.

The groundmass blue quartz varies from poly-crystalline and fine-grained, to monocrystalline and strained (undulose extinction, Figure 3c). The quartz typically has smooth, rounded contacts with the feldspars, and forms oval to subcircular grains. The polycrystalline quartz has grain boundary textures that range from sutured (unstable, Figure 3d) to metamorphic triple-point (stable). The sutured boundaries appear very similar to textures in Lower Roan arenites in drill hole IT28, and are probably related to Lufilian deformation. There is little consistent indication of the origin of its blue colour, either under the petrographic or the CL microscope, except that colour zoning in some grains is related to the internal distribution of polycrystalline versus monocrystalline quartz. This quartz is a common detrital component throughout the Lower and Upper Roan.

Biotite forms mm-sized to fine-grained flakes, some with inclusions of rutile that have optically darkened haloes, and is difficult to determine whether it is igneous or metamorphic/hydrothermal in origin: both grain sizes may be associated with epidote-clinozoisite.

Euhedral sphene is a common accessory in the groundmass, and shows no indication of alteration. Apatite forms euhdral to rounded tabular grains, and is very common in zones of clotted biotite-epidote, but rare within the feldspar phenocrysts. The apatite has a moderately strong greenish yellow luminescence, possibly indicative of Mn, and some grains are zoned. Magnetite is euhedral and occurs only within the altered plagioclase that mantles the phenocrysts. Minute grains of chalcopyrite also occur only within the altered plagioclase, where they are associated and locally enclosed within epidote (Figure 3e).

The phenocrysts are cut by minor veinlets of calcite, epidote, biotite, and rare chalcopyrite, that are locally continuous with the more pervasive alteration zones. This alteration-mineralization event is interpreted as Katangan or Lufilian in age.

Residual Basement (thin sections 82, 83)

The porphyry is separated from bedded, clearly sedimentary rocks by approximately 2.5 metres of dark, biotitic rock containing about 15% scattered pink feldspar phenocrysts and 15% blue-grey quartz grains, floating in a brownish-green matrix (Figure 4). The impression is one of a sedimentary rock derived very proximally from the porphyry.

In thin section, the feldspar phenocrysts and blue quartz grains are effectively indistinguishable from

Figure 2. KW-26, 553.3 m. Muliashi Porphyry. Note large k-feldspar phenocrysts mantled by greenish altered plagioclase, blue quartz, and dark biotite.

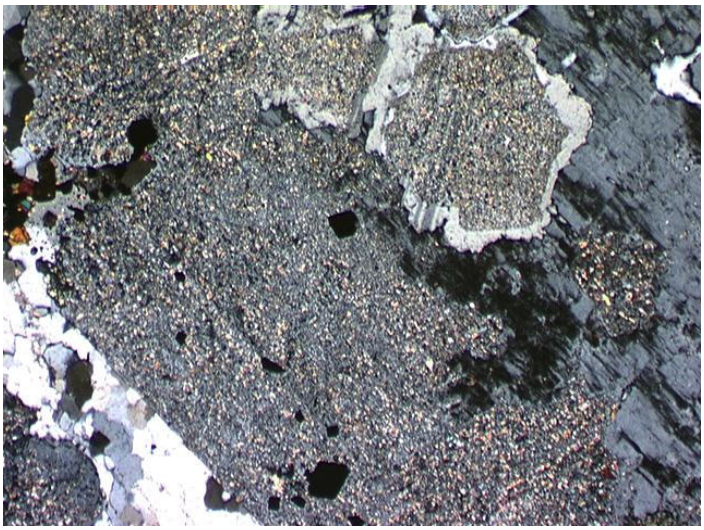

Figure 3a. TS81, cpl. View of edge of feldspar phenocryst, against polycrystalline quartz. Grey microcline overgrown by plagioclase, which is zoned from epidote-biotite altered, calcic cores to clear, unaltered, albitic rims. The phenocryst is mantled by altered plagioclase, which contains euhedral magnetite.

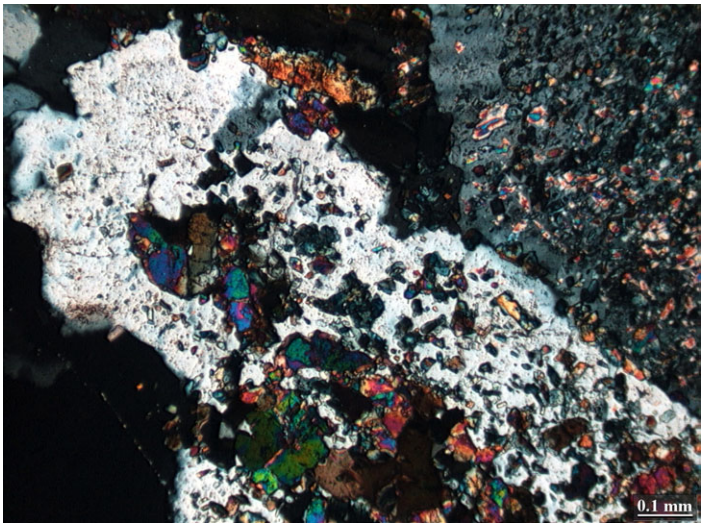

Figure 3b. TS81, cpl. Relatively coarse-grained epidote and clinozoisite, with associated biotite, replacing plagioclase.

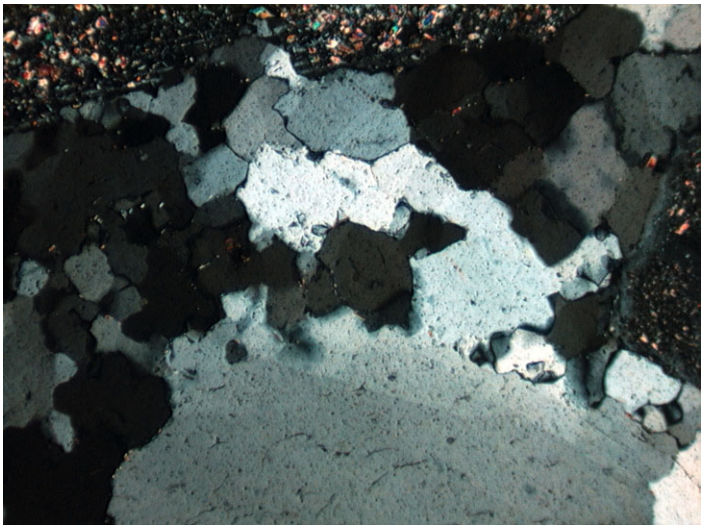

Figure 3c. TS81, cpl. Typical texture of polycrystalline quartz, on margin of large, 3-5mm blue quartz grain. Some grains show metamorphic triple-point boundaries, others are sutured, all show straight to almost-straight extinction. Core of grain is mono-crystalline, with undulose extinction.

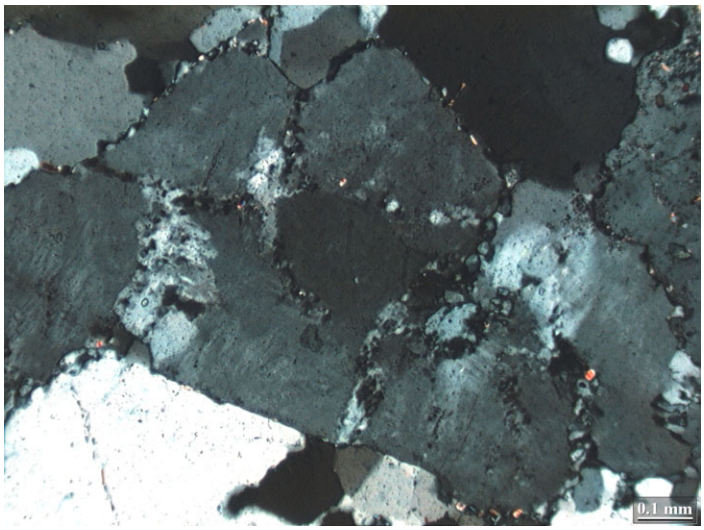

Figure 3d. TS81, cpl. Polygonal texture in microcline and quartz. The microcline is optically continuous, and dissected by thin seams of minute quartz-plagioclase-muscovite-biotite.

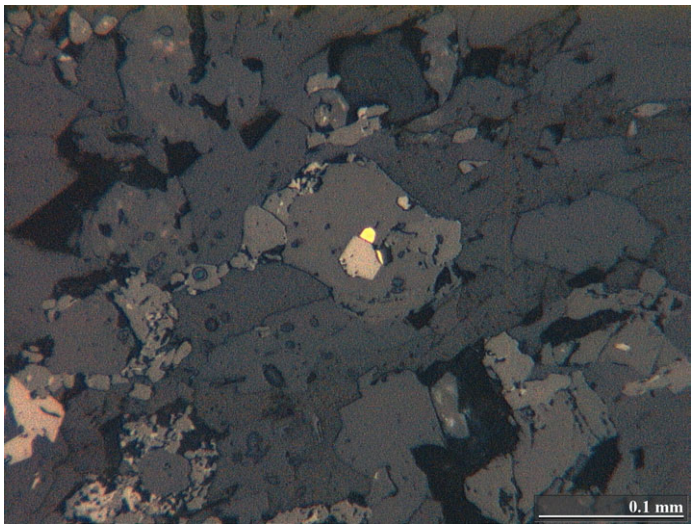

Figure 3e. TS81, reflected light. Chalcopyrite rimming rutile, within grain of epidote. Minor chalcopyrite is typically associated with epidote-biotite-(muscovite) alteration of plagioclase.

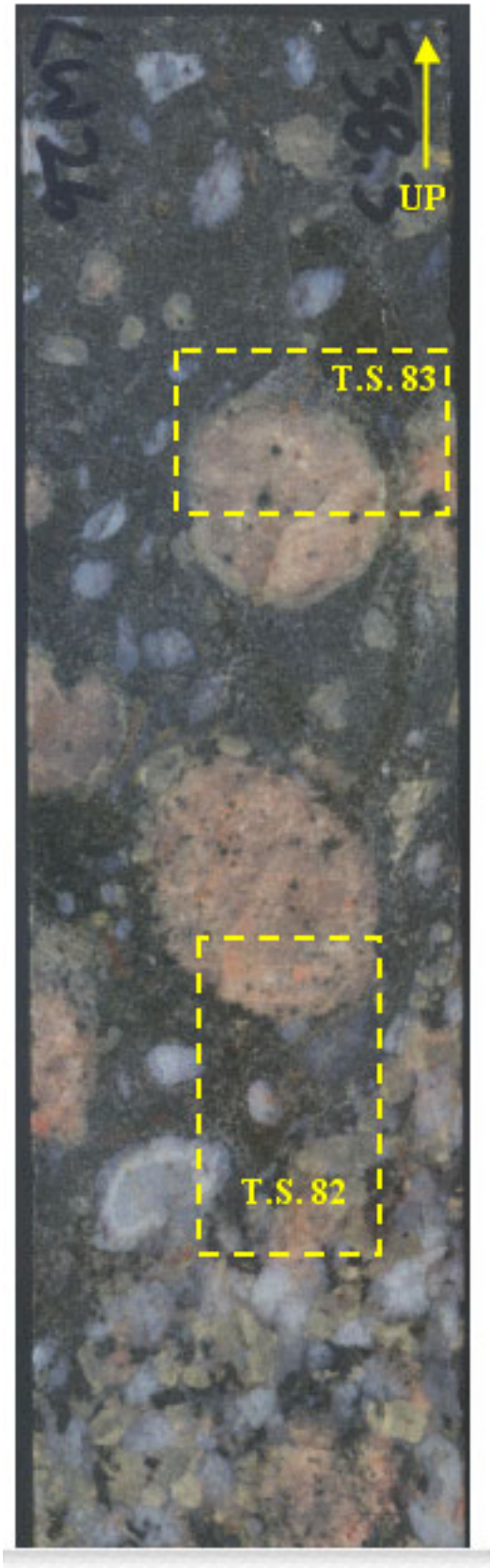

Figure 4. KW-26, 538.3 m. Regolith, Muliashi Porphyry. Intensely altered brownish matrix contains phenocrysts of k-feldspar, plagioclase and blue quartz.

those in the underlying sample. The perthitic k-feldspar phenocrysts are unaltered and shows no signs of (incipient) weathering, possibly because of its inherent stability (Figure 5a). In both thin sections the phenocrysts have a discontinuous halo of calcite-hematite-muscovite 1-2 mm thick, not seen in the unweathered porphyry. These same minerals occur locally in the groundmass, as irregular clots. Plagioclase phenocrysts are intensely altered to muscovite-epidote-clinozoisite-biotite (Figure 5b).

The brownish groundmass consists in thin section of 10 to 20% fine-grained biotite intergrown with 5 to 15% epidote-clinozoisite-muscovite, all overgrowing granitic-textured plagioclase and k-feldspar (Figure 5c). In most places the abundance of the secondary minerals prevents recognition of grain boundaries, and it is difficult to be certain whether the groundmass comprises large, eroded and transported porphyry fragments, or metamorphism of an in-situ residual porphyry. On the basis of the preserved igneous texture of the groundmass, the intact phenocrysts, the knowledge that phenocryst abundances vary widely within the Muliashi Porphyry (ie. 15% is not an unacceptably low abundance), and a comparison with the textures in the overlying bedded sediments, it is reasonable to interpret this as a metamorphosed residual porphyry.

The groundmass also contains sphene, ilmenite and hematite. Sphene forms subspherical detrital grains cored by ilmenite and locally apatite. The grains have a characteristic irregular, bumpy outline that is morphologically similar to the ubiquitous hematite grains in the Lower Roan sediments. Ilmenite occurs as bladed angular grains that are the likely precursor for the bladed, Ti-bearing hematite in the Lower Roan. Specular hematite forms pseudomorphs (martite) after euhedral magnetite, and lacks Ti.

The features of the residual zone suggest that weathering of the porphyry was accomplished by clay alteration of the feldspars, and oxidation of magnetite. The general lack of carbonate, silica or other infilling in the feldspars suggests that the secondary porosity created by clay weathering was not cemented, but preserved until later metamorphism to micas. Calcite, epidote-clinozoisite and biotite are common replacement products of the plagioclase, and also formed during metamorphism.

Lower Roan meta-sandstones and conglomerates (thin sections 84, 85)

Thin sections 84 and 85 are taken from bedded sandstone and conglomerate 10 to 20 cm above the weathered zone. In hand specimen the conglomerate contains obvious mm to cm-sized fragments of pink k-feldspar phenocrysts and blue quartz, within a sand matrix similar in composition to the sandstones (Figure 6). Graded bedding is absent or poorly developed and quite abrupt, and sorting is minimal. Outsized grains are commonly visible in the sandstones.

In thin section, the conglomerates are framework-supported with coarse sand to granule-sized grains of porphyry, feldspar and quartz, commonly with a moderate rounding (Figure 7a). In most cases this can be ascribed to the original texture of the porphyries (rounded feldspar phenocrysts and blue quartz), but other grains appear to have undergone significant transport. In particular, well-rounded quartz grains may be derived from other basement sources, most likely the Muva quartzites. Accessory grains of detrital muscovite are typically acicular and up to 1 cm in length, were not seen in the granites and also appear to have a different, unknown basement source (Figure 7b). The larger detrital grains occur within a framework of fine to medium-sized sand grains of angular to subangular quartz and feldspar, of clearly local origin. Also present are subspherical to broken, sand-sized grains of hematite, some of which show incomplete alteration from magnetite (Figure 7d-f). These are interpreted to have been derived from the primary magnetite and the zoned sphene-ilmenite grains in the granites. Rutile occurs as rare pseudomorphs after sphene, and more

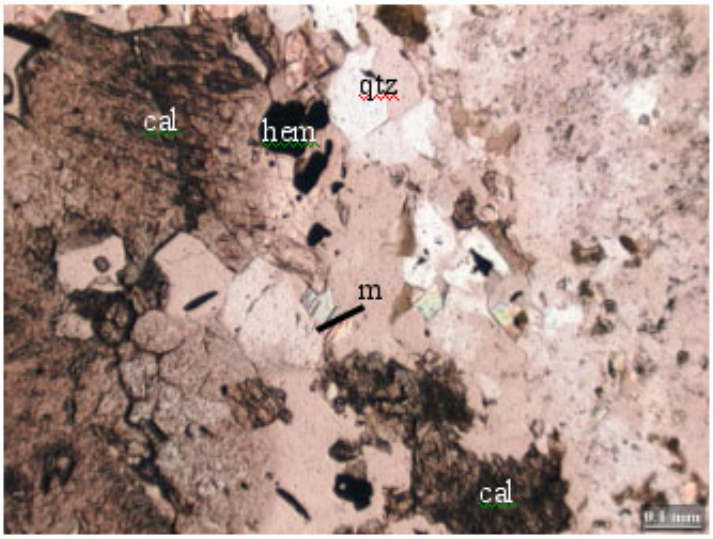

Figure 5a. TS82, ppl. Margin of large feldspar phenocryst (to right), with selvege of quartz, calcite, muscovite, hematite.

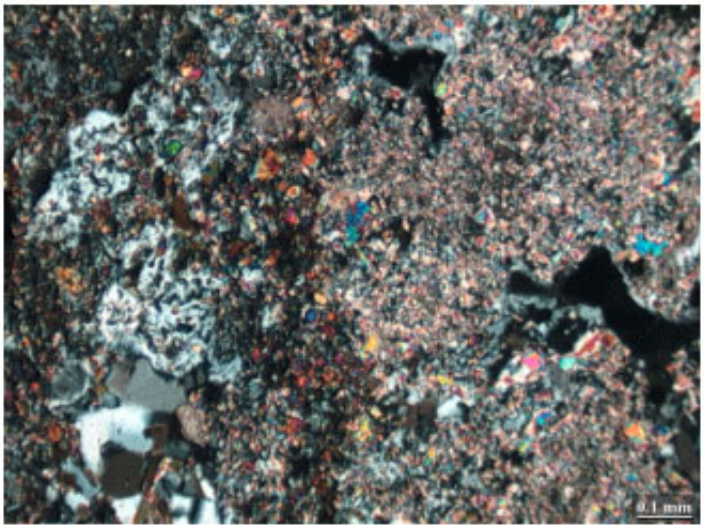

Figure 5b. TS83, cpl. Intensely altered plagioclase phenocryst, almost completely replaced by biotite-epidote-(muscovite). Dark grey interstitial quartz preserves original texture of phenocryst.

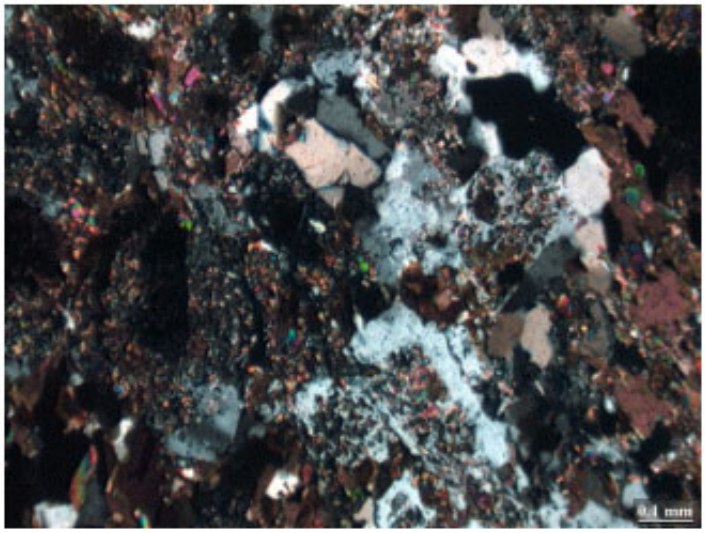

Figure 5c. TS83, cpl. View of groundmass to large feldspar phenocrysts. Groundmass has dark colour due to abundance of fine grained metamorphic biotite and epidote, but igneous texture is preserved. Interpreted as a metamorphosed residual granite.

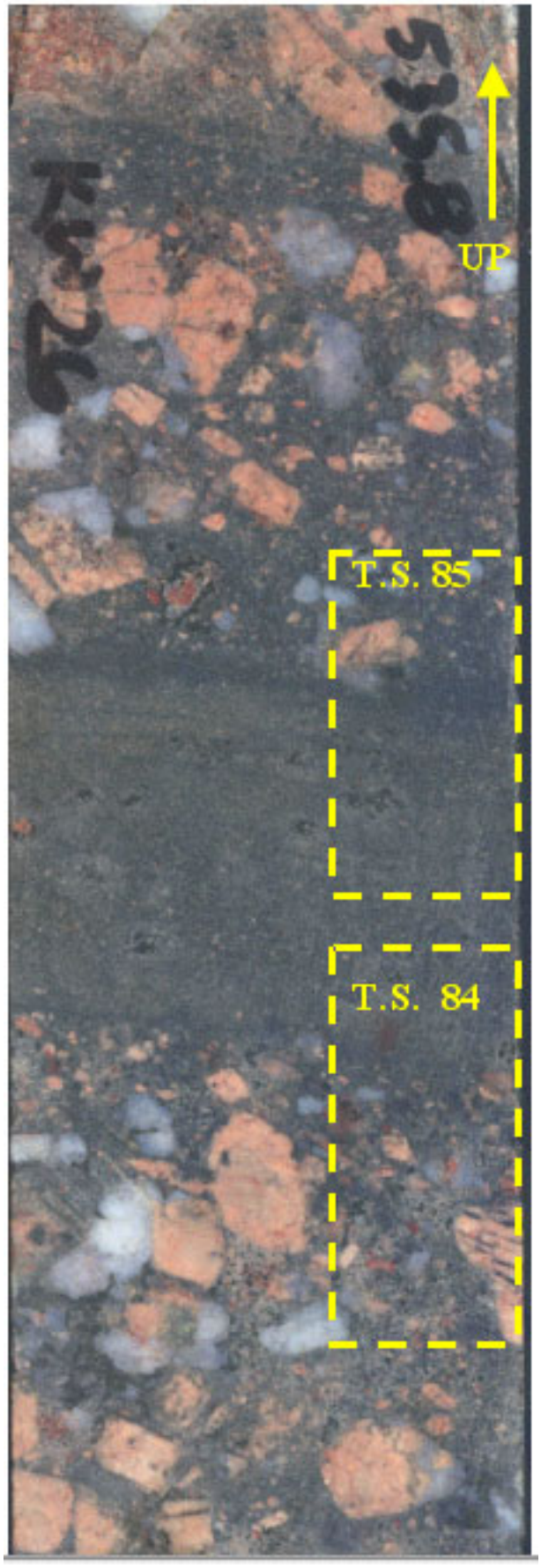

Figure 6. KW-26, 535.8 m. Lower Roan conglomerate and sandstone, 10cm above contact with porphyry. Note large angular granitic rock fragments, blue quartz and k-feldspar, poor sorting and lack of compaction textures.

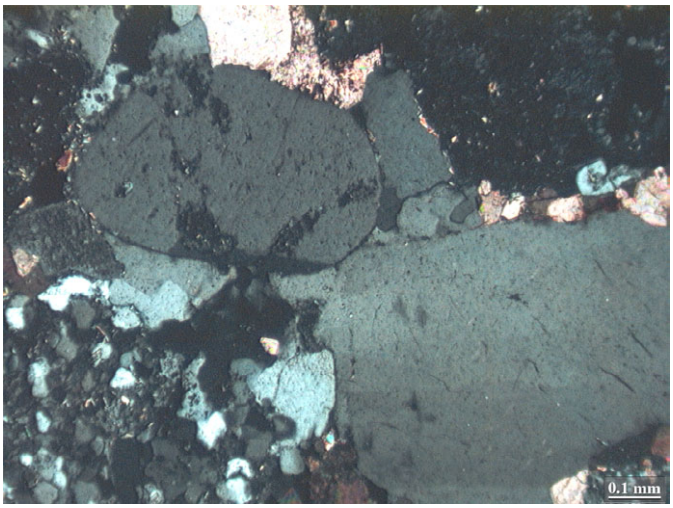

Figure 7a. TS84, cpl. View of framework grains in conglomeratic sandstone. Detrital k-feldspar (upper left) and quartz with biotite and Fe-Ti oxide dust rims, cemented by quartz.

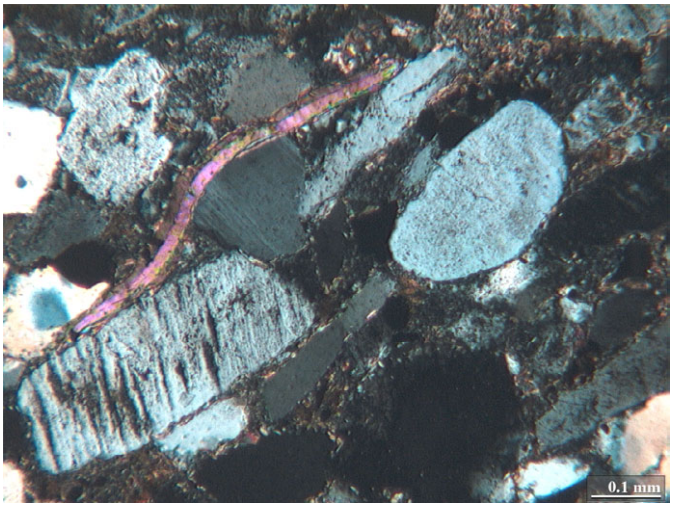

Figure 7b. TS85, cpl. Compacted arkosic sandstone, with bent detrital muscovite and well-aligned framework grains of quartz and feldspar. The matrix appears undeformed (although partly replaced by metamorphic biotite), there are no quartz or feldspar overgrowths, and the framework grains are unaffected by pressure solution.

Figure 7c. TS84, ppl. Fine-grained arkosic sandstone, subrounded and well-sorted framework grains. Bent detrital muscovite, partly mantled by metamorphic biotite, which also partly replaces the matrix. The cloudy k-feldspar grains have thin overgrowths of clear feldspar.

commonly as silt to clay-sized grains within the groundmass and coating detrital grains.

The estimated detrital composition of the conglomerates is 30 to 50% lithics (including porphyry, polycrystalline quartz), 25% quartz, 15% k-feldspar, 5 to 10% plagioclase, and accessory muscovite, and hematite. The conglomerate contains 5% to locally 10% silty matrix that under crossed polars has a fine mosaic texture and very low birefringence (Figure 7e,f), and is variably replaced by metamorphic biotite, muscovite or calcite. The SEM/EDS indicates that this matrix material consists largely of k-feldspar.

The sandstones contain a similar compositional range of detrital components, but intact porphyry rock fragments are rare. Framework grains are subangular to subrounded, the greater textural maturity due to elimination of the large lithic grains with roundness inherited from the porphyry. On average, the sandstones contain 40% quartz (monocrystalline), 30% feldspar (including 10% plagioclase), 5 to 10% lithics (porphyry, polycrystalline quartz), 1 to 2% detrital muscovite, 2 to 4% hematite, and about 1% rutile. The matrix comprises 5 to 20% of the rock, and is locally replaced by biotite, or calcite. The composition of the sandstone can be irregularly domainal on an intra-bed scale, such that they range in classification from lithic wacke to lithic arkose to feldspathic sandstone. This immaturity also occurs on an inter-bed scale.

Grain boundaries in both the sandstones and conglomerates are typically straight, smooth or curved, rather than sutured. Grains in the sandstone are most commonly floating or in contact with one or two other grains, and overgrowths occur on where grains are in contact (Figure 7c). A few of the detrital muscovite flakes are bent around quartz or feldspar grains, but there is otherwise little evidence of significant compactional deformation.

Overall, the sandstones show remarkably little evidence for cementation, dissolution and other diagenetic processes. In this regard it is noteworthy that the feldspar grains in the sandstone and conglomerate are no more altered to muscovite/biotite than in the samples of porphyry, possibly because the more weathered grains were destroyed during transport. More puzzling is the lack of either detrital or in-situ (ie. within plagioclase) epidote-clinozoisite in the sedimentary rocks, given their ubiquitous presence in the footwall granites. If these minerals represented a pre-Katangan metamorphic event, one would expect them to form part of the detrital record, particularly within large, intact granitic rocks fragments. If they represent a Lufilian hydrothermal/metamorphic event, which is suspected on the basis of their association with veining and chalcopyrite mineralization, their absence in the metasediments suggests a strongly localized control.

SEM/EDS work on the micas indicates that there are two end-member compositions present in the KW26 section. A pale, weakly to non-pleochroic, stubby lath-shaped mica with high birefringence is present in the plagioclase alteration, in calcite veinlets, and in mantled zones around feldspar phenocrysts in the residual zone. It contains little or no Ti, no Cl and is low in Mg, but has significant Fe. It is likely an Fe-bearing muscovite. The second mica is a brown, pleochroic, biotite that also occurs in the plagioclase alteration and veinlets, as well as in the residual granite groundmass, in nodules or clumps of coarser biotite, and as a mantle to the hematite and detrital muscovite. It contains considerably more Fe than the pale mica, as well as significant amounts of Ti and Cl. Coarse-grained biotite associated with mineralization in the Konkola drill hole KLB145 also tends to be elevated in Fe, Ti and Cl. More work needs to be done to confirm this association, and may help constrain the type and pathways of mineralizing fluid.

Ndola East Area, Drill Hole IT28

A series of drill holes some thirty years ago tested the area around the present-day Ndola Lime

operation, several of which passed into a gneissic basement. Unlike the Konkola area, the thickness of the Lower Roan beneath the Ore Shale is remarkably consistent between holes, such that individual beds immediately above the basement contact can be correlated over several kilometres. The depositional setting appears to have been tectonically much quieter from that at Konkola. Although all of the holes contain copper mineralization, its grade is consistently sub-ore (<2%). The contact is also interesting because the gneissic basement appears to contain "windows" of Lower Roan sandstone and it is not obvious that an erosional contact exists.

In hand specimen the contact between the gneiss and the sandstone parallels the orientation of poorly defined layering within the sandstone, as well as the orientation of a hematite-bearing vein in the gneiss (Figure 8). The gneissic layering lies almost perpendicular to these features, and is abruptly cut by the contact with the sandstone. Unlike the basal sandstones described from Konkola, the sandstones here are even-grained, dark, and contain no material obviously derived from their immediate footwall.

The sandstone consists in thin section of more than 90% quartz with less than 10% feldspar (microcline and accessory plagioclase), accessory biotite and hematite, and rare zircon, and hence is a quartz arenite (Figure 9a). The framework grains are well-sorted, and mud or silt-sized matrix is absent. The rock has a striking sutured texture, which along with a moderately developed preferred orientation of grains indicates strong pressure solution parallel to bedding (the basement contact). This is supported by the rarity of preserved dust rims of Fe-Ti oxide and mica (clay) dust rims (Figure 9a). However, their presence indicates a period of early diagenetic oxidation similar to that at Konkola.

The arenite gradually decreases in average grain size and sorting towards the contact with the gneiss, coincident with a gradual increase in the abundance of suture-lining fine-grained biotite, and of sutured, and in many instances stylolitic grain boundaries (Figure 9 b). These changes may reflect a change in the original sediment toward a more poorly-sorted, feldspathic arenite, with slightly higher clay content expressed as grain coatings.

The sutured texture could be interpreted as related to diagenetic pressure solution during burial. However, the texture occurs locally within the underlying gneiss (Figure 9d), and in the hematite-bearing plagioclase-calcite-quartz-biotite vein. Together these suggest that the sutured texture developed, or was at least modified, during metamorphism-deformation.

The contact with the gneiss is indistinct to irregular on the thin section scale. The uppermost part of the gneiss consists of large quartz, feldspar and quartz-feldspar intergrowths that define the steep gneissic texture, separated by zones of fine-grained sandstone similar to that above the contact (Figure 9c). Hematite is much more abundant below the contact, and forms large, mm to cm-sized irregular grains within the sandstone. The texture could be interpreted as being due to sandstone deposited within steep cracks penetrating the basement, or, alternatively, as a metasomatic overprint upon the sandstone. However, dark, mosaic-textured, k-feldspar-quartz matrix occurs locally within the gneiss, supporting a framework of detrital grains, and indicates a sedimentary origin (Figure 9e).

Two types of biotite occur, a fine-grained biotite that overgrows the matrix and detrital feldspar and contains rutile, and a younger, coarse-grained biotite that lacks rutile and mantles late, clear plagioclase (Figure 9f). The younger biotite is texturally similar to the coarse biotite found in mineralized nodules. Further SEM work is required to characterize the different generations of biotite.

Vein hematite appears to have formed (or remobilized) late in the paragenetic sequence, because it truncates and brecciates sutured quartz and the vein infilling minerals, albite, k-feldspar, and calcite. Vein minerals show evidence of deformation prior to

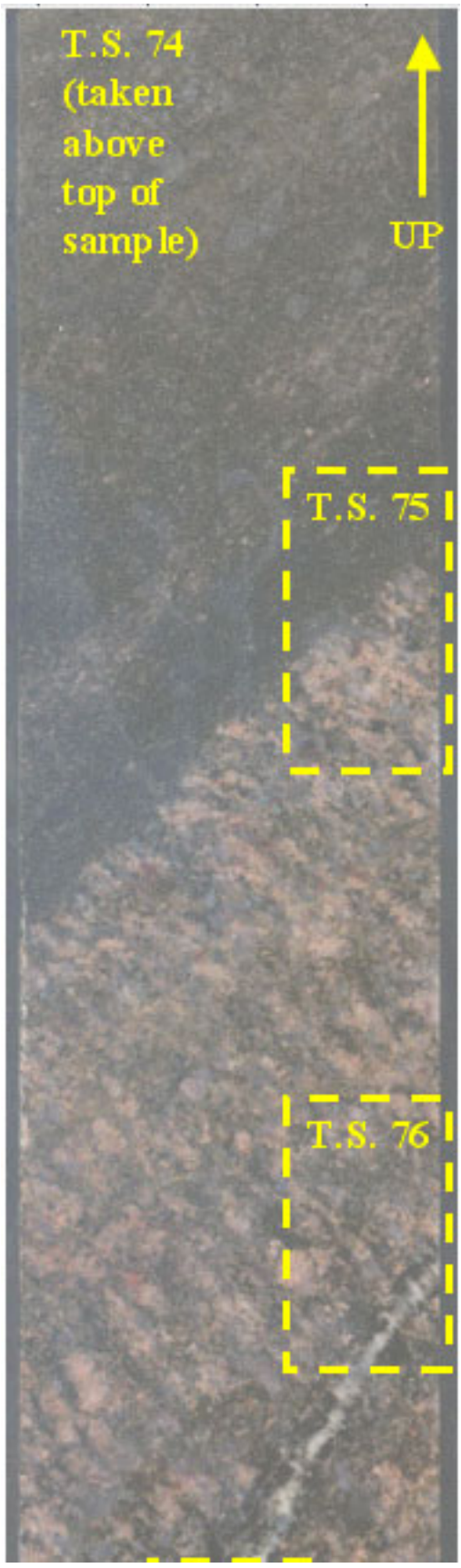

Figure 8. IT28, 5098 ft. Contact between Lower Roan quartz arenite and basement "gneiss". Note faint layering in arenite parallel to the contact and to the hematite vein, high angle "gneissic" banding in basement.

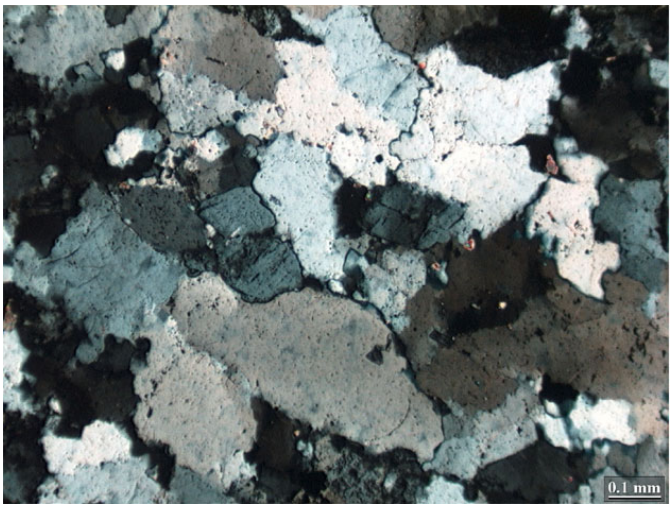

Figure 9a. TS74, cpl. View of part of thin section furthest above the basement contact. Quartz arenite, with locally preserved dust rims showing original detrital texture, largely obliterated by extensive pressure solution. Preferred orientation of grains subparallels the basement contact. Note lack of matrix – originally a clean sand.

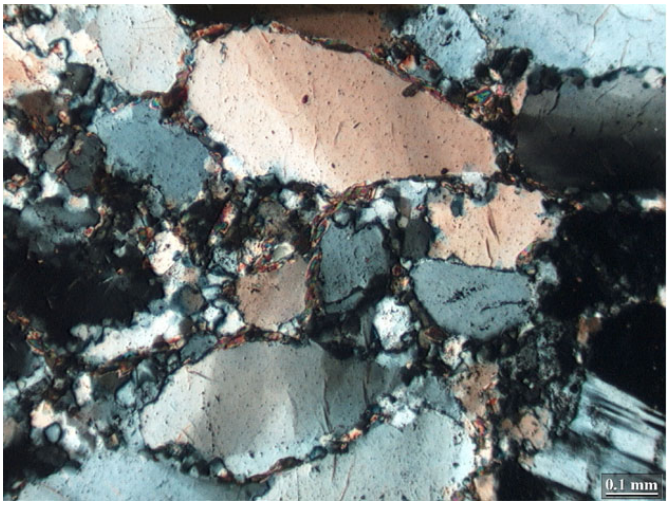

Figure 9b. TS74, cpl. Sample closer to the basement contact than (a), with more intense suture development associated with higher biotite content.

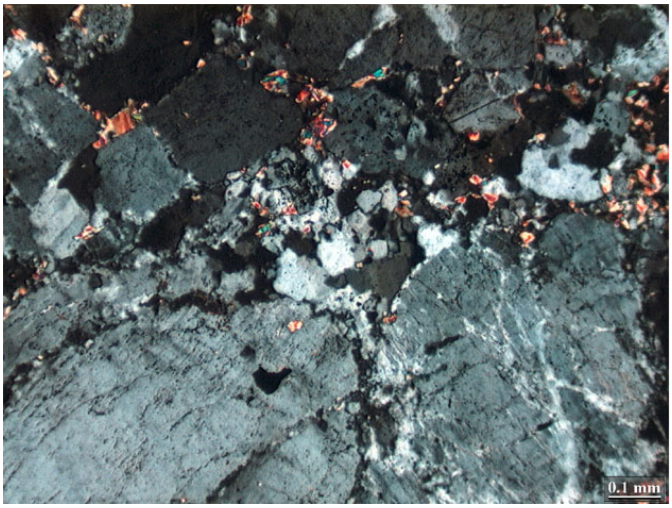

Figure 9c, TS75, cpl. View immediately inside basement contact (trends NW-SE immediately left of slide), long dimension of large feldspar grains perpendicular to contact. Basement consists of large granitic fragments with intervening zones of sand-sized detrital grains, and interstitial biotite.

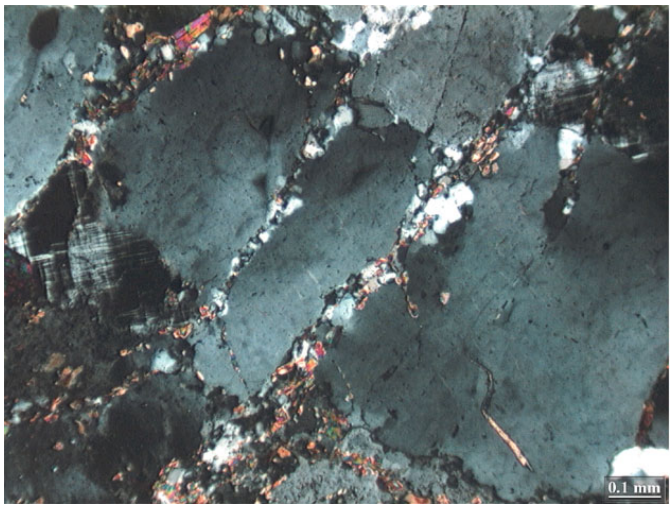

Figure 9d. TS76, cpl. Large quartz grain cut by quartz-plagioclase-biotite veinlets, compositionally similar and parallel to pressure solution seams and sutured texture in overlying sandstones. Also parallel to large veinlet of albite-quartz-biotite-carbonate-hematite.

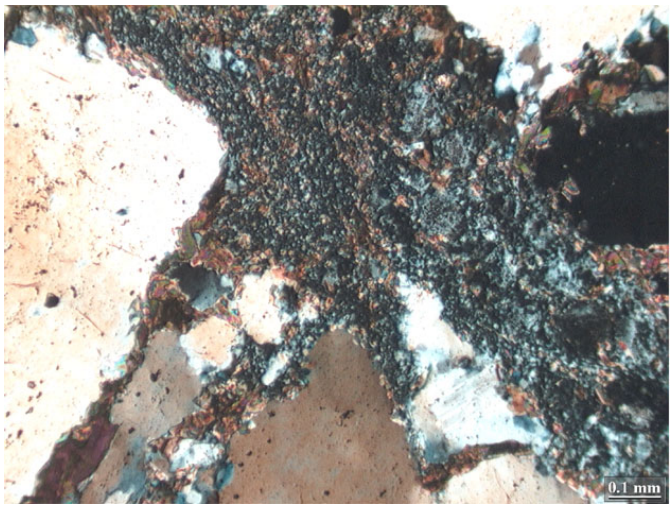

Figure 9e. TS76, cpl. Dark cherty matrix partly overgrown by biotite, surrounding large and locally broken grains of quartz, feldspar.

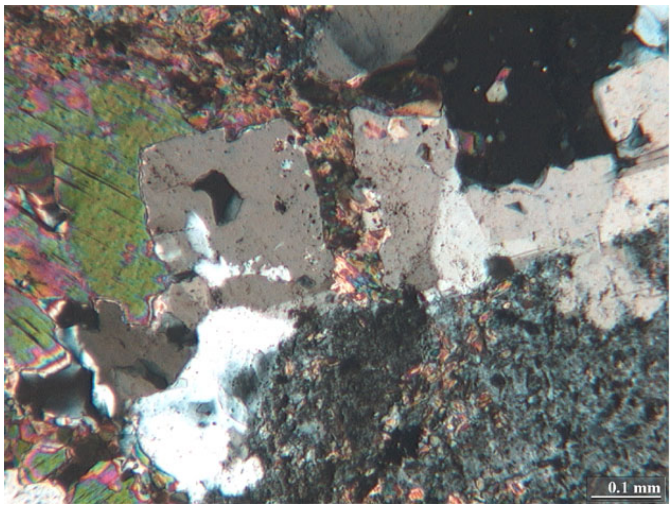

Figure 9f. TS78, cpl. Detrital / residual granitic fragment of dark k-feldspar partly overgrown by biotite, mantled and replaced by clear subhedral plagioclase. Two generations of biotite are present – a fine-grained biotite with dark rutile, and a coarse-grained biotite that lacks rutile and mantles the euhedral plagioclase.

truncation by hematite, such as kink bands in albite, undulose extinction and suture development in quartz. The timing and morphology of the vein hematite is similar to that of the vein-associated sulfides, and they may be temporally related. Clear, twinned albite occurs in the veins and locally around their margins, and in one instance demonstrably overgrows an earlier detrital k-feldspar grain (Figure 9f). Sodic alteration is apparently absent at Konkola, but is here seen to be associated with hematite mineralization.

Summary and Conclusions

The basement – Lower Roan contacts in the Konkola East (Kawiri) and Ndola East areas contain transitional zones where igneous textures are partially preserved yet sedimentary features are also present. These zones are interpreted as metamorphosed regoliths. At Kawiri, the transition is characterized by intense biotite-epidote alteration of the feldspars, taken to reflect original weathering of the granite. At Ndola, the transition is marked by high-angle fractures filled with sediment from the overlying sandstone.

Plagioclase in the Muliashi porphyry is altered to epidote-biotite-(muscovite-calcite), which also forms thin veinlets and carries minor chalcopyrite. This mineralization is interpreted to be associated with Lufilian deformation, on the basis of its similarities with late Ore Shale mineralization. Significant zones of basement-hosted mineralization such as at Samba may well be Lufilian, rather than pre-Katangan, and would not provide a copper source for the Lower Roan ore bodies.

The early diagenetic features of the Lower Roan rocks are remarkably consistent between these widely spaced locations, specifically the presence of oxides and clays coating detrital grains. Pressure solution is strongly developed in the Ndola basal sandstones, but is also present in the gneiss, and is likely related to deformation rather than burial diagenesis. Weathering of the basement rocks may locally be preserved as a regolith, but feldspars in the overlying sandstones are no more visibly weathered than in the basement.

The granites contain sphene that is a source for the detrital/authigenic rutile and ilmenite in the Lower Roan. Magnetite occurs in the granites but is associated with the epidote-biotite alteration, and so may be secondary. Hematite in the Lower Roan is likely derived from replacement of ilmenite, and the metamorphism of amorphous iron oxides. The peculiar blue quartz characteristic of the Roan sedimentary rocks is granitic in origin.

Biotite in both the basement and sedimentary rocks has two forms, small, groundmass biotite that is locally associated with or encloses rutile, and coarse biotite flakes that are paragenetically late. Similar coarse biotite is elsewhere associated with mineralization. Albite is mantled by the coarse biotite and formed at an earlier stage, and also occurs in calcite-hematite veins. Sodic alteration is important at a few Katangan deposits, but is not consistently developed in the Copperbelt ore bodies.

Comparative Study of Drill Cores from the Konkola North Orebody and Barren Gap

David Broughton
Colorado School of Mines

Summary

This report describes detailed petrographic and textural features from a mineralised intersection of Ore Shale (DDH KLB145 – Konkola #3 orebody) and two barren Ore Shale intervals (DDH KLB67 from the Konkola barren gap, and KLB83 on the eastern fringe of #3 orebody). In KLB67 the mineralized intersection occurs within interbedded feldspathic arenites, feldspathic greywackes and siltstones, but is best developed within the sandstones. Mineralization displays a marked zoning from a central, high-grade, bornite-chalcopyrite zone of ferroan dolomite-(biotite) alteration and abundant veining, through a proximal, lower grade, biotite-muscovite zone with chalcopyrite prevalent over bornite, to a distal zone of biotitemuscovite with rutile but no sulfides. Cobalt is present throughout the sulfide zone but most abundant occur in the lower, dolomite-poor interval. The lithologies in KLB67 are identical to those in the mineralized zone and this suggests the barren gap is not lithologically controlled. The sandstone and siltstones in the barren gap appear to have undergone the same diagenetic history, with early oxidation and weathering recorded by dust rims of Fe-Ti oxides and micas (clays), followed by later diagenetic K-feldspar and quartz overgrowths. Bedding-parallel veinlets, predominantly composed of carbonate, are present in KLB67, but are much less abundant than in the mineralized zone. A brief examination of DDH KLB83 intersection indicates it is similar to the barren gap.

Introduction

The Konkola area lies at the northwestern end of the Zambian Copperbelt, and consists of two ore bodies continuous at depth, the South or No. 1 ore body and the North or No. 3 ore body (Figure 1). The ore bodies are separated by an unmineralized "barren gap" nearly 1.5 km wide at surface, that extends to a depth of approximately 600 m. Below this the ore bodies merge, such that on a longitudinal section the gap forms a U-shaped zone. The gap was encountered early in the drilling delineation of the deposit, and not surprisingly was tested by few surface holes. The Konkola barren gap presents an opportunity to compare stratigraphically equivalent mineralized and unmineralized rock units, in a part of the Copperbelt that generally appears relatively undeformed.

Little is documented about the geology of the barren gap, or of the nature of its boundaries with the ore bodies. Fleischer et al. (1976) describe it as follows: "approaching the gap from the north orebody, ore is restricted to the C unit [note – the mine geologists subdivide the Ore Shale into five units, from base to top A through E, see Table 1] and lenticles of sandy dolomite increase in frequency and the shale layers between the thickening dolomites are crumpled and folded… cherty quartz lenses become more abundant in the dolomite bed and in the weathered formation form "quartz rubble" … it may be suspected that an algal bioherm occupies part of the unexplored barren gap…". Sweeney and Binda (1989) mention it only in passing as a "presumed bioherm", and the current mine geologists also regard it as such.

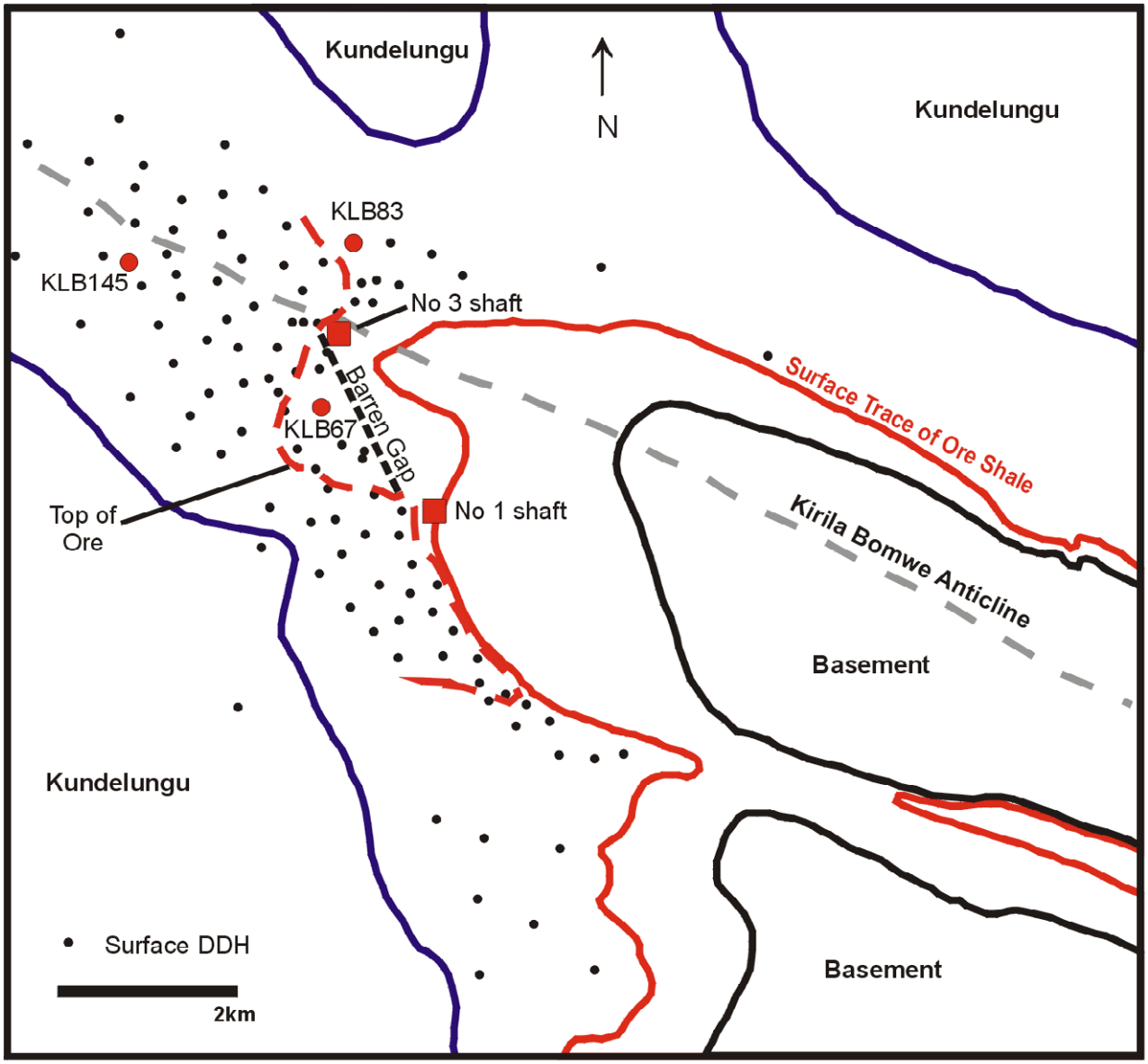

Figure 1. Simplified geology of the Konkola area, Northern Copperbelt, showing Konkola surface drill holes, location of the No. 1 (South Orebody) and number 2 (North Orebody) shafts, vertical projection of the orebdies, and position of the barren gap. Collar locations for the three holes used in the study are highlighted.

A review of logs and preserved cores from the early surface holes through the barren gap indicated that the shallower intersections were in weathered ground unsuitable for study, and that the deeper intersections contain no significant carbonate. There is no "algal bioherm" at Konkola. A brief underground visit to the north ore body–barren gap transition area confirmed in general terms the above description of the transition: the abundance of carbonate increases southwards and mineralization (predominantly bornite) occurs selectively in the carbonate bands. Over a lateral distance of less than 25 m the approximately 4 to 7 metre-thick combined C and D carbonate-banded units changed from 10 to 20% to approximately 50% carbonate. Individual bands commonly change in thickness across asymmetric NE trending folds (Figure 3a). Unfortunately, drift development had stalled and was soon afterwards terminated due to ground conditions, so that the transition from this high grade, bornite-carbonate zone to the unmineralized and carbonate-poor barren gap was not exposed.

This study compared drill cores through the Ore Shale in the North Orebody (KLB145) with unmineralized intersections from the barren gap (KLB67) and from a drill hole immediately east of the north ore body (KLB83) (Figure 1). The Konkola mine stratigraphic terminology is used for reference. Samples with secondary copper mineralization were excluded from the study, in order to focus on hypogene mineralization controls. Petrographic observations were augmented by cathodoluminescence (CL) and scanning electron microscope (SEM) studies.

Konkola North Ore Body, Drill Hole KLB145

Drill hole KLB145 intersected the north ore body on the south limb of the northwest-plunging Kirila Bomwe Anticline, approximately 2.6 km from drill hole KLB67 (Figure 1). In this area the rocks strike southeast and dip southwest at 25–30°. The Ore Shale was intersected from 680.0 to 692.0 m, and is underlain by 8 m of Footwall Conglomerate, followed by 1 m of Footwall Sandstone in which the hole was stopped at 701.0 m depth. Mineralization above 1% Cu is confined to Ore Shale units A through D, and consists of hypogene sulfides (chalcopyrite, bornite, carrolite) throughout all of the zone but the lowermost

Table 1 Konkola Ore Shale Stratigraphy (modified from Sweeney and Binda, 1989)

Member, Unit	Thickness	Description
Hangingwall Quartzite (HWQ)	10 - 150m	Interbedded feldspathic arenite, greywacke, and minor siltstone
Ore Shale, Unit E (OSE)	0.6 - 1.5m	Interbedded siltstone and subordinate feldspathic arenite
Ore Shale, Unit D (OSD)	1 - 3m	Interbedded siltstone and dolomitic/calcareous feldspathic arenite, with bedding-parallel carb-qtz-Cu veinlets
Ore Shale, Unit C (OSC)	0.9 - 4m	Interbedded siltstone and dolomitic/calcareous feldspathic arenite, with bedding-parallel carb-qtz-Cu veinlets
Ore Shale, Unit B (OSB)	1.4 - 2m	Massive to laminated sandy siltstone
Ore Shale, Unit A (OSA)	0.6 - 1m	Finely laminated siltstone
Footwall Conglomerate (FWC)	0 -20m	Polylithic, poorly sorted conglomerate and interbedded coarse sandstone; usually leached.
Footwall Sandstone (FWS)	<40m	Poorly sorted feldspathic, lithic sandstone/greywacke; usually leached.
Porous Conglomerate (PC)	<40m	Polylithic, poorly sorted conglomerate, leached.

1.1 m of unit A. This lower portion of the zone is weathered, and it contains predominantly secondary copper minerals. The underlying footwall conglomerate and sandstone are also weathered and contain sub-ore grade secondary copper mineralization. Sampling from this intersection was limited to six quartered cores, from which nine polished thin sections were prepared.

Figure 2 summarizes the geology, alteration, mineralization and assay results from the mineralized section of KLB145. The best mineralization coincides with a central zone of dolomite-biotite alteration and dolomite-veining in units C and D. Together these comprise 6.5 m of the 11.5 m intersection and have an average grade of 3.4% Cu, compared with 1.7% Cu for the remaining 5 m. Cobalt values in the carbonate-rich units are approximately one-half that of the lower units B and A.

In the following section, a general description of the lithologies and mineralization will be followed by observations from petrographic study.

The footwall sandstone is a red to olive brown, massive to poorly bedded, coarse-grained greywacke or muddy sandstone, and may represent an interbed within the footwall conglomerate unit. The conglomerate is polylithic, massive bedded, unsorted, matrix- to locally clast-supported, with a coarse sandstone matrix and local cm to dm sandstone interbeds similar to that of the footwall sandstone. Both units are characterized by patches of red-weathered carbonate and hematite, and minor malachite-chrysocolla-chalcocite. The contact with the overlying Ore Shale (OS) is sharp and bedded.

The lowermost unit of the OS, from 692.0 to 688.4 m, consists of a massive-bedded, brownish (weathered), very fine-grained sandstone to siltstone that coarsens slightly upwards. It corresponds with the mine units A and B. The uppermost metre is finely laminated (Figure 3b) and is gradational to the overlying unit (C). Chalcopyrite occurs as disseminated grains, bedding-parallel lenticles and minor veinlets, along with malachite, chalcocite and local native copper below 689.0 m. Bornite is rare to absent. Carrolite is intergrown with chalcopyrite in the veinlets.

From 688.4 to 684.25 m the OS consists of cm to mm bedded, grey, fine- to coarse-grained dolomitized sandstone and siltstone. This unit occurs within the mine subunit C. Chalcopyrite and bornite occur as disseminated irregular grains, lenticles and veinlets, both parallel and oblique to bedding (Figure 3c). The veinlets contain fibrous quartz, ferroan dolomite and copper sulfides, which define a consistent down-dip (~WSW) lineation. In thin section some of the veinlets also possess a weak crenulation fabric. Ferroan dolomite is most intensely developed as halos to the veinlets.

From 684.25 to 681.5 m (~units C and D) the OS consists of very fine to medium grained dark grey dolomitized sandstone interbedded on a centimetre to millimetre scale with pale grey dolomitized siltstone. The dolomite is associated with and forms haloes around bedding-parallel veinlets of ferroan dolomite-quartz-bornite-chalcopyrite (Figure 3d). Bornite and chalcopyrite are roughly equivalent in abundance. The upper contact of the dolomitic zone is sharp (Figure 3e), and coincides with a lithological change from arenite (dolomitized) to greywacke.

The uppermost unit of the OS extends from 681.5 to 678.5, and consists of a coarsening upwards sequence of interbedded sandstone and siltstone. Although the mine log placed the upper contact of unit E at 680.0 m, the contact between the OS and the HWQ is gradational and rather arbitrary, and here placed at the base of a prominent coarse-grained sandstone bed. Disseminated chalcopyrite and lesser bornite extend upwards from the dolomitic zone to 680.6 m (Figure 3f), above which the OS is barren of sulfides.

The HWQ consists of pink to grey, massive medium- to coarse-grained feldspathic sandstone and cm to dm thick bands of dark greenish to brownish grey siltstone. Hematite occurs above 676 m as disseminated grains and rare bedding-parallel

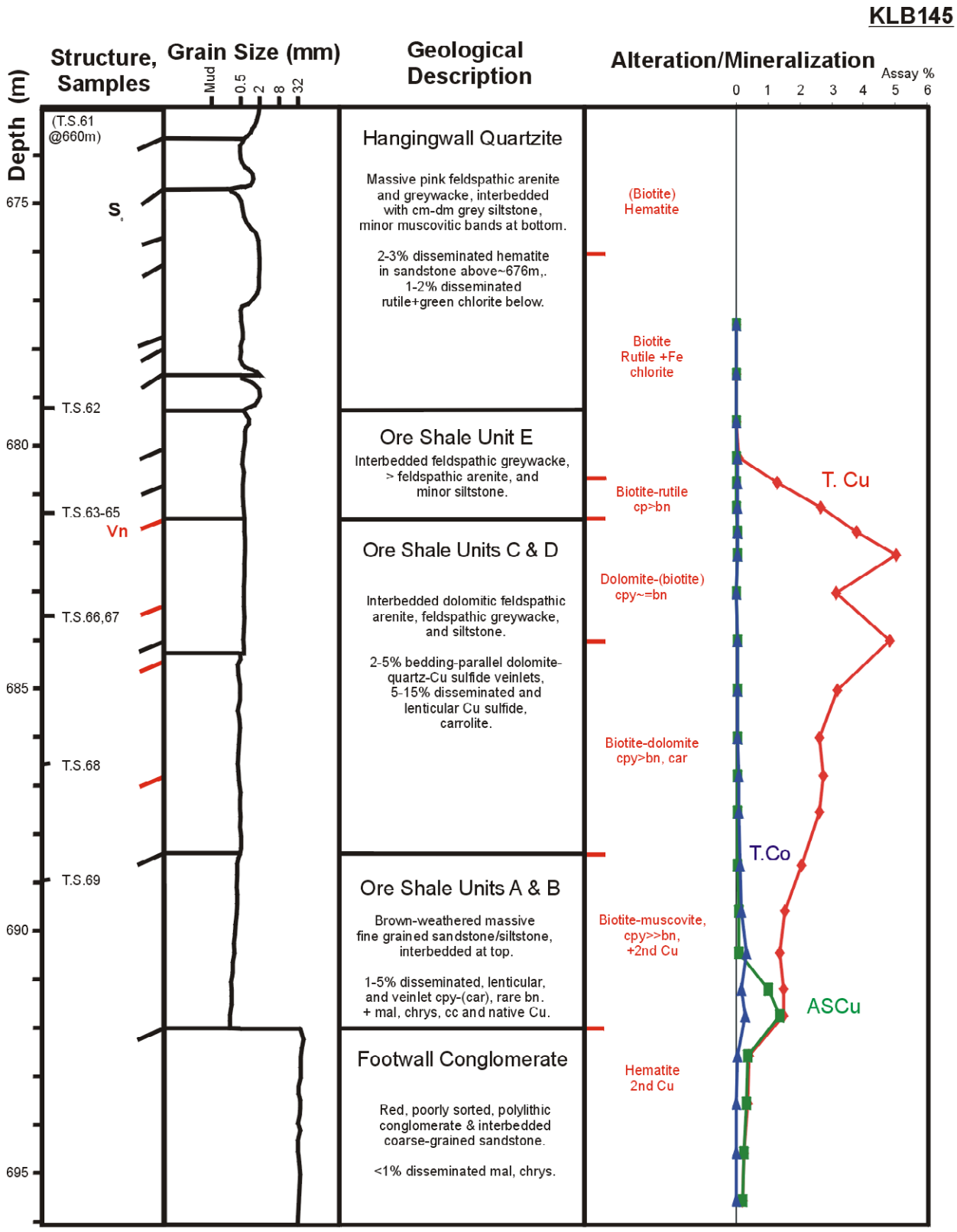

Figure 2. Summary graphical log of lower part of drill hole KLB145, Konkola North orebody. Note zoning of alteration-mineralization around central veined unit C+D. Upper contact of Cu +dolomite controlled by contact between veined arenite and overlying greywacke (unit E).

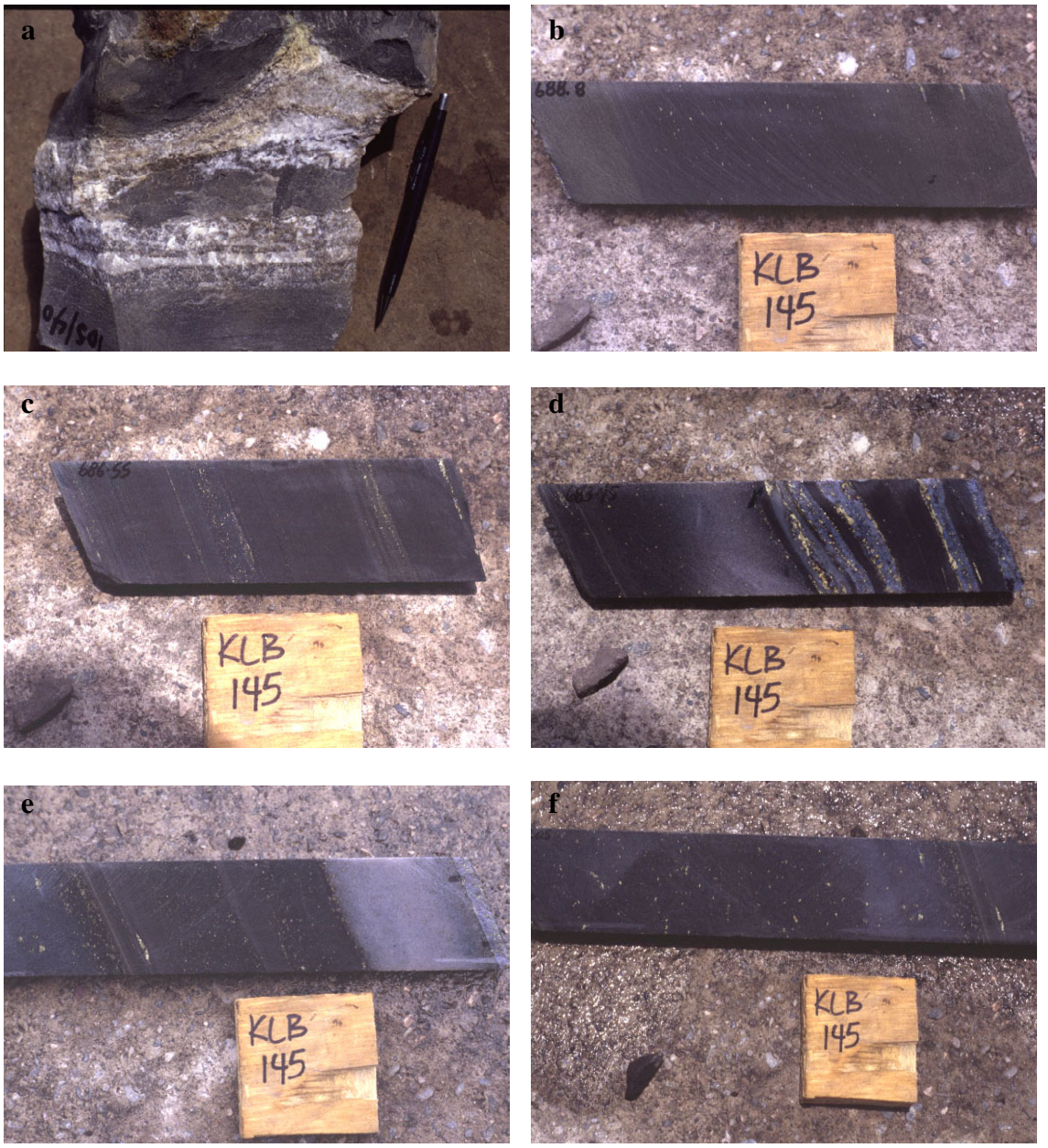

Figure 3. (a) Oriented sample from southern margin of Konkola North orebody, near barren gap, viewed to NE. Dolomite-bornite bands thicken SE (toward barren gap) across NE trending asymmetric fold structures. (b) sample of unit B, 688.8m, massive siltstone with disseminated sulfides. (c) sample of unit C, 686.55m, dolomitic sandstone-siltstone with banded / veinlet and disseminated sulfides. (d) sample of unit D, 683.45m, of bedding-parallel ferroan dolomite (stained) – sulfide veins. (e) contact between unit E (left) and unit D, dolomitized arenite. (f) sample of unit E at 681m, note disseminated sulfides, lack of carbonate. All core samples approximately 5cm across.

concentrations, the latter associated with pinkish colouration.

In thin section, the sandstones and siltstones have well-preserved sedimentary and diagenetic textures, although tectonic fabrics are developed locally. The OS rocks are composed of subrounded to rounded detrital framework grains of quartz, k-feldspar, muscovite-altered feldspar, muscovite (large platy grains), minor granitic and cherty rock fragments, and accessory apatite and zircon. In most specimens these are poorly sorted, and occur within a matrix of fine silt to clay-sized k-feldspar, quartz and muscovite. The matrix, detrital muscovite and k-feldspar are variably overgrown by biotite and fine muscovite. Sulfide and oxide textures are described below.

The sandstones vary texturally between matrix-supported greywackes and matrix-poor feldspathic arenites. In the arenites, the grains are in mutual contact, may show evidence of pressure solution, and quartz and feldspar overgrowths and cement are common, often preserving dust rims of Fe-Ti oxides and mica after clay (Figure 4a, b, h, see also Figure 6c, k). Quartz cement is relatively common in the arenites, and locally has undulose extinction, suggesting it pre-dates Lufilian deformation. In the greywackes, detrital grains are less commonly in mutual contact, and overgrowths of quartz and feldspar are rare or absent (Figure 4c, d).

The distribution of matrix-rich and matrix-poor sandstones appears to be an important control on the distribution of carbonate and sulfide mineralization. The top of carbonate alteration at 681.5m is coincident with the contact between an overlying greywacke and the underlying feldspathic arenite (Figure 2, 3e). Dolomite in the altered arenite occurs as discrete grains overgrowing feldspar, biotite, matrix and possibly quartz (Figure 4g, h). In addition, mineralization is preferentially developed within sandstones rather than siltstones, as can be seen in its overall distribution (Figure 2) as well as on the thin section scale (Figure 4i).

A distinct zoning exists across the OS, both in alteration and sulfide mineralogy (Figure 2). The central zone (units C & D) is characterized by bedding-parallel dolomite-chalcopyrite-bornite-(quartz, biotite, k-feldspar, apatite) veinlets, ferroan dolomite-(biotite) alteration and approximately equivalent amounts of disseminated bornite and chalcopyrite (Figure 3d, 4g, h). Biotite is destroyed where dolomitization is most intense. This central zone contains the high grade mineralization and "carries" the entire interval . It is enveloped by a zone of less intense, biotite-dolomite alteration and fewer veinlets, where chalcopyrite is more abundant than bornite. This interval also contains visible carrolite in the footwall of the central zone. The outermost mineralized zone consists of biotite and generally fine-grained muscovite alteration, rare to absent veinlets, and, especially in the footwall, chalcopyrite much more abundant than bornite. The footwall zone also contains more abundant carrolite.

The Lower Roan hangingwall and footwall of the mineralized interval are characterized by minor biotite alteration and ubiquitous, widespread specular hematite, both as disseminated grains and in veinlets. The hematite facies is separated from the mineralized interval by a zone of biotite-(muscovite)-rutile-Fe chlorite (Figure 2, 4a,b).

Sulfide textures are distinctive, and in some instances similar to those of hematite in the stratigraphically equivalent barren intersections. Hematite is absent within the mineralized zone, however, clusters and individual minute grains of rutile are present in trace to accessory amounts, and are locally intergrown with biotite (Figure 4e,f) or mantled by Cu sulfide (Figure 4l). In most instances rutile appears to have formed prior to Cu sulfides, probably during diagenetic oxidation (dust rims). Chalcopyrite and bornite are mutually intergrown, or chalcopyrite occurs as rims and fracture-related infillings or replacements of bornite. Pyrite is absent. The Cu sulfide grains generally vary in grain size according to the grain size of their host rock, however a wide

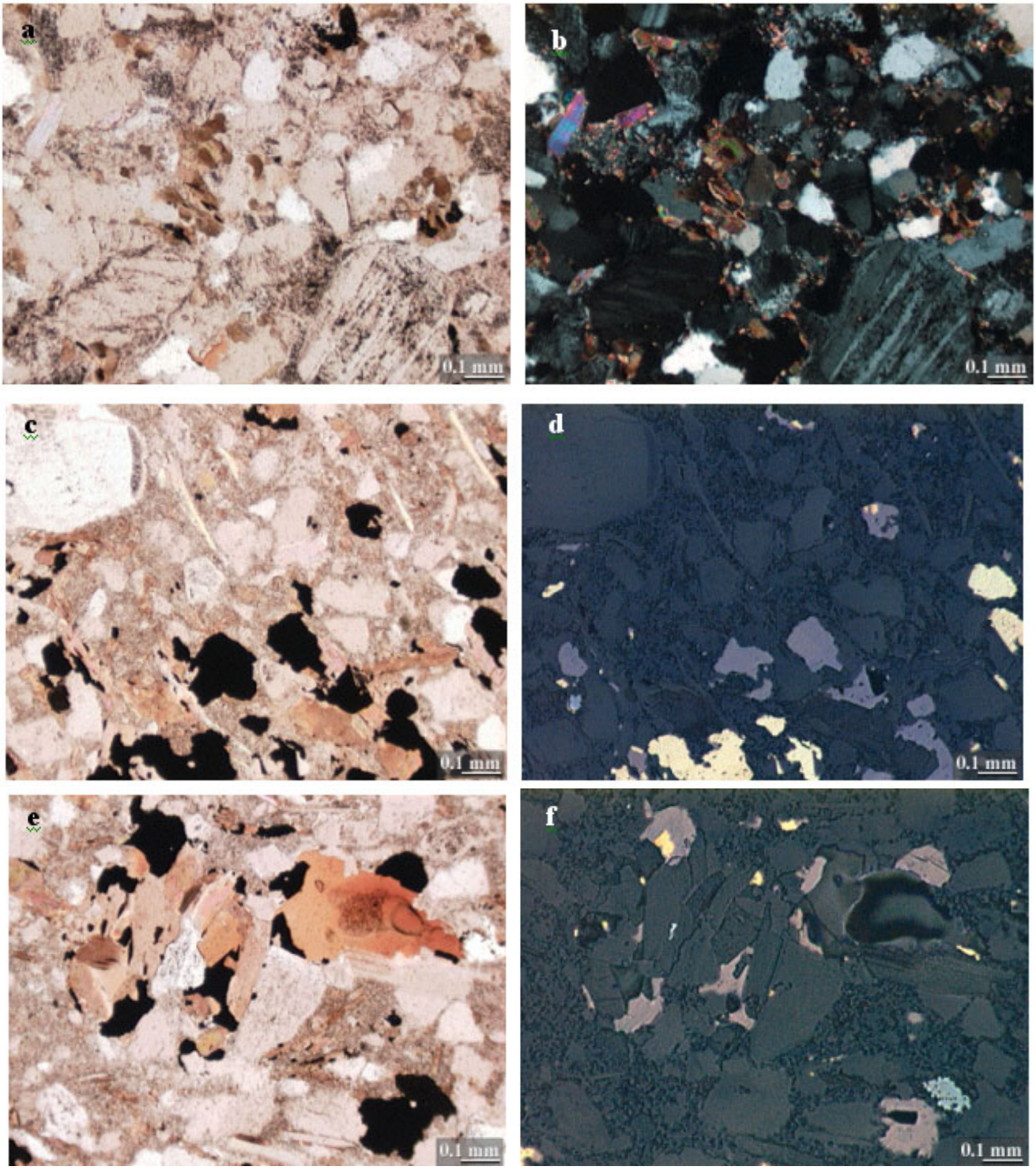

Figure 4, KLB145 photomicrographs, showing zoning and textures of alteration-mineralization across the OS. (a,b) TS62, feldspathic arenite with biotite+muscovite alteration, rutile. (c,d) TS63, above dolomitic zone, feldspathic greywacke with biotite alteration, chalcopyrite-bornite. (e,f) TS63, "nodule" of biotite-bornite around detrital k-feldspar; bornite is late, rutile (bright grey) is enclosed in biotite (left center) and early – also note rutile separate from bornite in lower right.

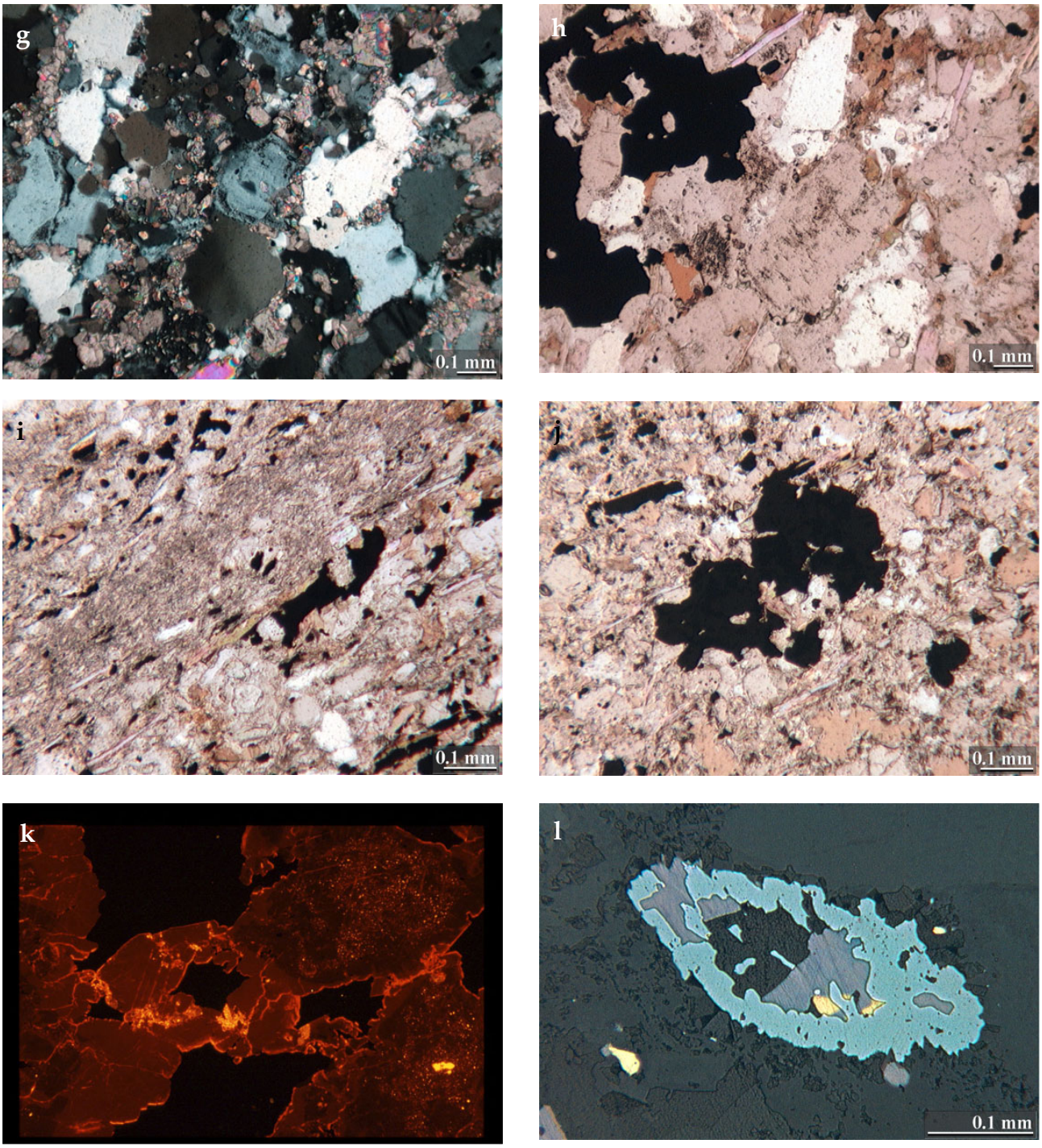

Figure 4 cont'd. (g). TS64, dolomite alteration replacing k-feldspar overgrowths in feldspathic arenite. (h) TS64, coarse chalcopyite-bornite and dolomite-biotite alteration in well-cemented feldspathic arenite. (i) TS67, bedded sandstone-siltstone, biotite-(dolomite) alteration and Cu sulfides predominantly in sandy layers. (j) TS69, coarse, irregular chalcopyrite in muscovite-(biotite) alteration at base of OS. (k) TS67, CL, dolomite-chalcopyrite veinlet, zoned from speckled ferroan to dark red ferroan to bright yellow-red (manganoan?) dolomite, and youngest chalcopyrite; field of view 2mm. (l) TS63, rutile (bluish) probably after sphene, filled with biotite (dark grey) and bornite-chalcopyrite.

range exists and the largest sulfide grains are always much coarser than the detrital silicates. Chalcopyrite and bornite are most commonly found in direct association with biotite and dolomite, with which they form small grain aggregates, nodular structures and in the central zone, veins (Figure 4 c-f). Similar nodular structures containing anhydrite were described elsewhere at Konkola (Sweeney and Binda, 1989), and were interpreted as sulfide replacement features after diagenetic (evaporitic) anhydrite nodules. Anhydrite was not observed in any of the three holes examined, but where seen elsewhere in the district usually occurs in structurally late sites (veins).

Morphologically, the disseminated sulfide grains vary from subspherical but non-rounded (eg. very irregular at the grain boundary scale), to lenticular or platy (particularly where developed within biotite), to highly irregular (Figure 4). Copper sulfide grains are observed to mantle or partly replace detrital silicate grains and their overgrowths, apatite overgrowths, and dolomite. Within and adjacent to veins, Cu sulfides typically brecciate dolomite and quartz, and fill open space between the non-sulfide minerals (Figure 4k). This range of textures can be seen in both the dolomite-altered and non-dolomite-altered zones, although the altered zones generally contain a greater proportion of outsized and irregular grains. This suggests that all of the copper sulfides record the same mineralization event associated with the veins and the dolomite-biotite alteration. The overall impression is one of sulfide precipitated or remobilized late in the paragenetic history, as the final phase in vein filling, replacement of matrix, detrital grains and diagenetic overgrowths, and as grains nucleated on and replacing earlier oxides.

Sweeney and Binda (1989) described brown-luminescent feldspar overgrowths on normal, blue-luminescent k-feldspar within the OS, and documented elevated Cu contents (~0.25% Cu) within some of these overgrowths. They interpreted these features as a critical piece of evidence for Cu being present within the (diagenetic) fluid that caused the overgrowths. Both clear and cloudy k-feldspar and k-feldspar overgrowths were noted during the current study. In many clouded grains the clear feldspar persists along cleavage into the grain core, and in this type "dust rims" of Fe-Ti oxides and mica are absent. In contrast, some of the clear feldspar grains have oxide-mica dust rims that pre-date the cloudy overgrowths. The clear and clouded feldspar do not show any compositional variation with semi-quantitative SEM/EDS. There was no indication (SEM) of elevated Cu content in the overgrowths, and, in contrast, some of the overgrowths and detrital grains are clearly mantled and partly replaced by paragenetically later Cu sulfides. Sweeney and Binda noted malachite in their samples, and included it as part of the diagenetic sequence, and it is suspected that their samples were affected by relatively recent secondary copper formation, as is prevalent in many parts of the mine.

Cathodoluminescence study of the alteration and vein carbonates demonstrated a complex paragenetic history of changing Fe and Mn contents. The matrix carbonate grains are commonly cored with rhombs of ferroan dolomite, which is successively overgrown by dolomites of generally lower iron content. A distinctive yellow luminescent carbonate is commonly present roughly midway through the sequence, and is likely related to elevated Mn content. These overgrowths are preserved within coarse-grained, dark to bright red luminescent dolomite and/or calcite, that forms mosaics of interlocked grains whose overall morphology is unrelated to the earlier zoned carbonates. A similar progression is observed in veins, where early, finely zoned carbonates are enveloped within younger, texturally simple, dark to bright red luminescent dolomite (Figure 4k). This confirms a genetic link between the matrix and vein dolomites.

In summary, the mineralized intersection occurs within interbedded feldspathic arenites, feldspathic greywackes and siltstones, but is best developed within the sandstones. Mineralization displays a marked zoning from a central, high-grade, bornite-

chalcopyrite zone of ferroan dolomite-(biotite) alteration and abundant veining, through a proximal, lower grade, biotite-muscovite zone with chalcopyrite prevalent over bornite, to a distal zone of biotite-muscovite with rutile but no sulfides. Cobalt is present throughout the sulfide zone but most abundant occur in the lower, dolomite-poor interval. The mineralized zone is enveloped within widespread specular hematite mineralization, of probable earlier age. Diagenetic overgrowths of quartz and feldspar are present in the arenites, and trap earlier diagenetic Fe-Ti oxides and micas.

Konkola Barren Gap, Drill Hole KLB67

Drill hole KLB67 intersected the Ore Shale midway between the North and South ore bodies, at a depth of 211.7 to 219.3 m (Figures 1, 5, 6a). Core angles indicate a true thickness of 7.2 m, about 4 m less than in KLB145. Assay results for the intersection range from 0.03 to 0.06% TCu for all but the lowermost 1.3 m, which averaged 0.11% TCu and 0.04% ASCu. Mineralization was not observed in the core, and it is suspected that the minor Cu values are related to fine-grained secondary copper.

The hole ended in 7.5 m of interbedded pinkish to pale conglomerate and coarse-grained feldspathic sandstone (Porous Conglomerate, PC), overlain by 14.8 m of red to grey to beige, massive bedded, and very coarse-grained feldspathic sandstone (Footwall Sandstone, FWS, Figure 5). Both of these units contain up to 3% disseminated and bedding-parallel specular hematite. The Footwall Conglomerate is missing in this hole, such that the OS lies directly upon the FWS. This suggests that the OS – FWS contact is an unconformable surface, correlative with the base of the OS and/or the base of the FWC. The distribution of the FWC is irregular on the scale of the deposit, and unrelated to the location of the barren gap.

Each of the five subunits of the OS are present in KLB67, which suggests depositional continuity between the mineralized and barren OS "stratigraphies" - placed in quotation marks because the OS stratigraphy is partly defined by the abundance of dolomite veinlets and alteration. The combined lowermost subunits, A and B, are 1.8 m thick and comprises a buff-weathered to dark grey-green very fine-grained sandstone/siltstone. They are overlain by 6.7 m of dark green-grey fine to very fine-grained sandstone, interbedded with up to 10% discontinuous mm to cm bands of medium to coarse-grained dolomitic feldspathic arenite (subunits C and D). Bedding-parallel veinlets of dolomite-quartz-specular hematite and disseminated specular hematite are almost exclusively confined to the lowermost 1.4 m of this zone. The OS is capped by 0.8 m of dark grey fine-grained sandstone interbedded with approximately 5% cm-thick beds of coarse-grained feldspathic sandstone, and up to 5% green-grey siltstone (subunit E).

The OS is overlain by a thick hangingwall sequence of cm- to dm-interbedded red-brown feldspathic greywackes and sandstones, and dark green-grey very fine-grained sandstone/siltstone, locally with "grit", that contain prominent disseminated specular hematite. Although quartz and feldspar overgrowths are present in the three thin sections made of these sandstones (Figure 6c, d), they are generally poorly cemented. The amount and distribution of cement affects permeability, and could play a role in controlling the subsequent movement of mineralizing fluids. For instance, well-cemented hangingwall or footwall rocks could form seals to cross-stratal fluid migration, and barren gaps could develop where cementation was poor, or dissolved prior to mineralization.

Thin sections were made of two samples from the FWS, 0.3 and 5 m below the unconformable OS contact. Both consist of matrix-poor feldspathic lithic sandstones with rounded to subrounded detrital k-feldspar, quartz, granitic and chert rock fragments, cemented by quartz and k-feldspar overgrowths. Abundant porosity (up to 30%) exists in both samples, and is defined predominantly by mm-sized, generally rounded but irregular shaped holes. There is no Cu

KLB67

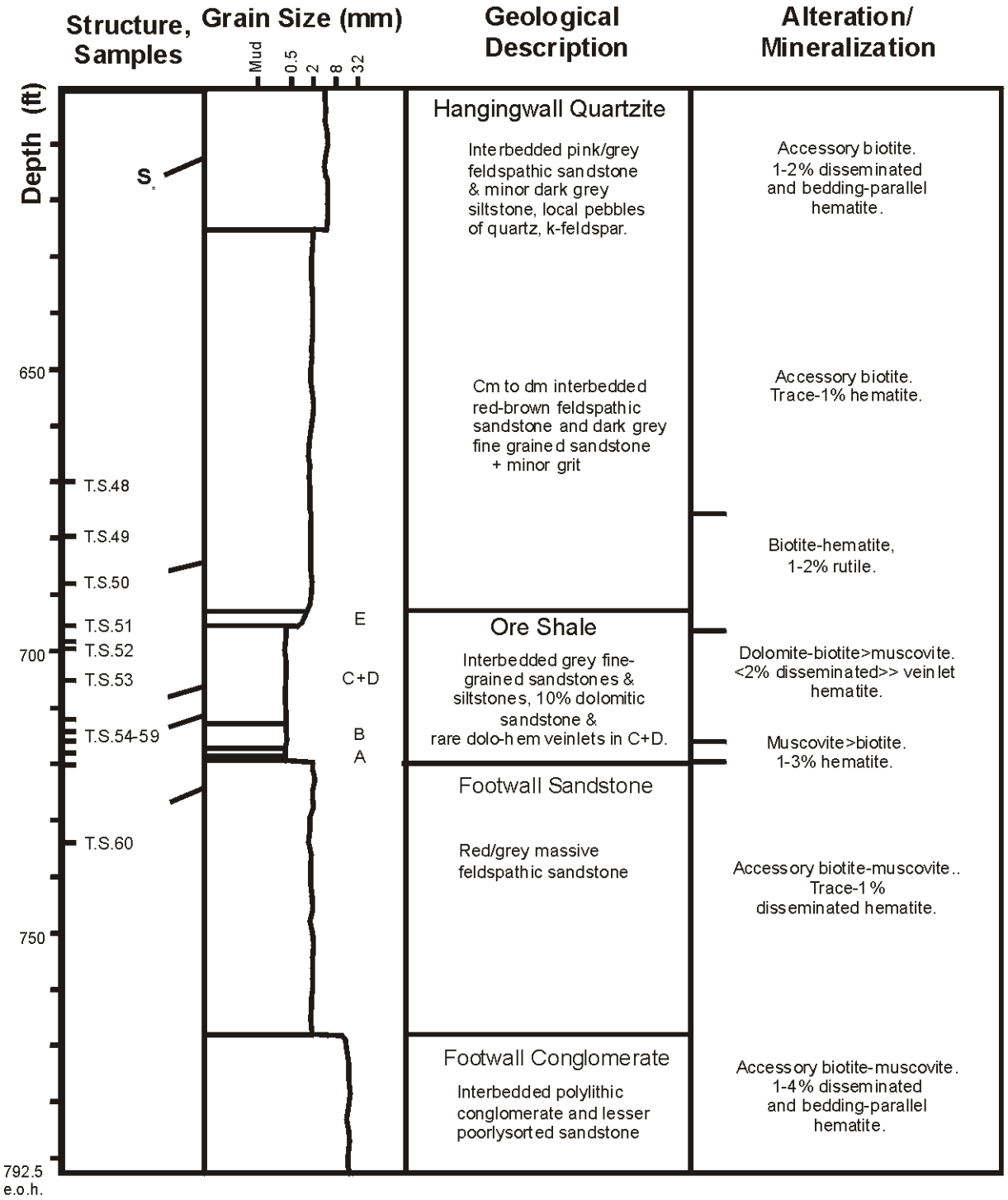

Figure 5. Summary graphical log of lower part of drill hole KLB67, in Konkola Barren Gap. Note zoning of dolomite-biotite-muscovite alteration.

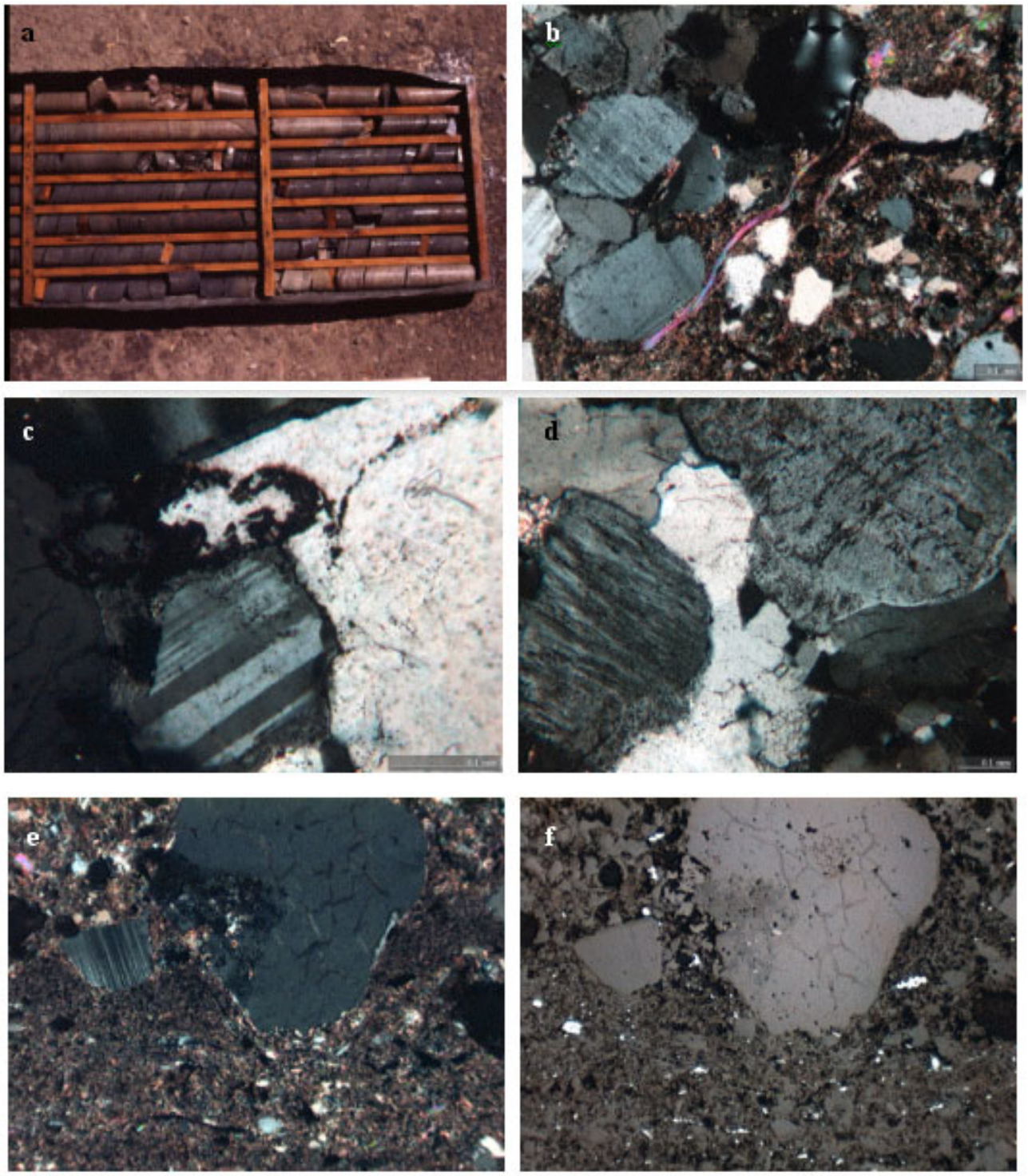

Figure 6, KLB67 and KLB83. (a) KLB67 barren gap intersection of Hangingwall Quartzite, Ore Shale, and Footwall Sandstone. (b) KLB67, TS48 (HWQ), contact between feldspathic arenite and feldspathic greywacke, note detrital (bent) muscovite. (c) KLB67, TS50 (HWQ), quartz overgrowths trap early dust rims of rutile-hematite-(mica)n and a rutile pseudomorph after sphene. (d) KLB67, TS50 (HWQ), quartz cement after earlier k-feldspar overgrowth. (e,f) KLB67, TS51, Ore Shale E – D transition zone, contact between siltstone and pebbly arenite, hematite (reflected light) is fine-grained, after ilmenite / amorphous Fe oxides, notable lack of coarse grained hematite at contact.

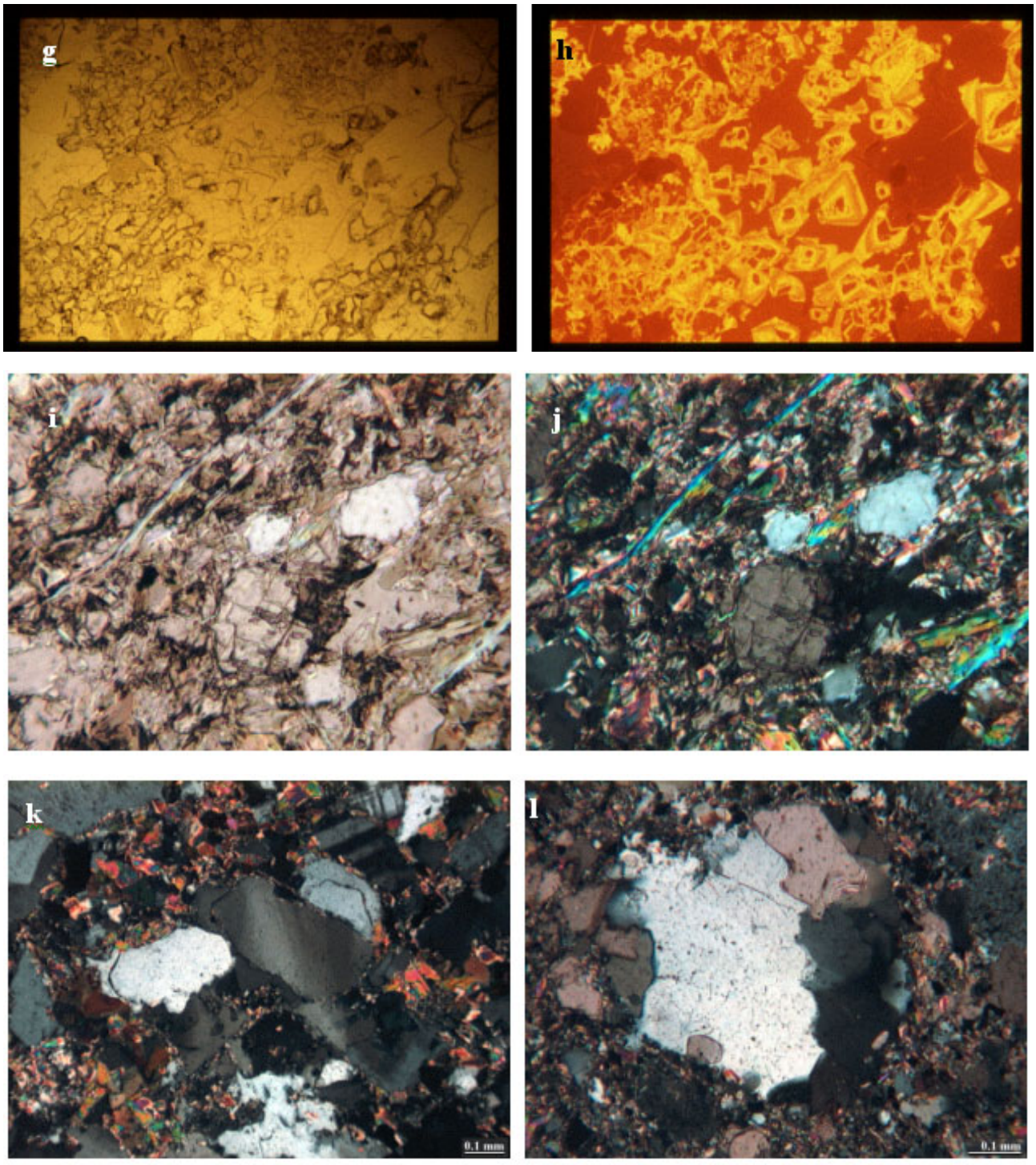

Figure 6, cont'd. (g,h) KLB67, TS52 (OSD), plane light and CL views of dolomite-(hematite) veinlet, with early zoned Fe/Mn rhombohedral dolomite and late, space-filling red-luminescent ferroan dolomite. (i,j) KLB67, TS53 (OSC), dolomite-biotite-muscovite (fine-grained) alteration and minor opaque hematite in feldspathic arenite. (k) KLB83, TS70 (HWQ), quartz overgrowths preserve diagenetic hematite-rutile-mica (clay) dust rims, hydrothermal/metamorphic biotite in groundmass. (l), KLB83, TS72 (FWS), ferroan dolomite alteration of groundmass and detrital quartz.

or Fe staining associated with the holes, as might be expected were they leached sulfide grains. Detrital feldspar and quartz grains show no signs of dissolution and are therefore unlikely to be the origin of the porosity. This texture is common throughout the OS footwall and, to a lesser degree, hangingwall rocks in the Konkola area, and may be caused by dissolution of carbonate or sulfate.

In thin section, the original sedimentary composition and morphology of the barren gap lithologies appear identical to those in KLB145. The sandstones are poorly sorted with up to 20% matrix, and contain detrital k-feldspar, quartz, muscovite and lithic fragments as described above (Figure 6b). The siltstones contain only rare lithic fragments, and a greater abundance of muscovite, but are otherwise similar to the sandstones.
The detrital quartz, feldspar and lithic grains in the sandstones are commonly coated with "dust rims" of biotite and muscovite (after clay), hematite and rutile, preserved by k-feldspar and quartz overgrowths (Figure 6c, d). The quartz is more abundant and locally forms a cement that post-dates the authigenic feldspar. The quartz cement often shows undulose extinction and recrystallization, and therefore pre-dates at least part of the Lufilian deformation.

The matrix, detrital muscovite and to a minor extent the k-feldspar grains and overgrowths are variably overgrown by metamorphic/hydrothermal biotite. The biotite is commonly intergrown with, or partly replaced by dolomite, and also contains specular hematite and local rutile along cleavage planes.

Hematite most commonly occurs as disseminated platy and subangular to rounded, originally octahedral grains up to 1 cm in size (Figure 6e, f). The octahedral grains are composed of partly to completely martized magnetite and ilmenite, and locally preserve octahedral cleavage and skeletal habits. SEM/EDS study indicates that the hematite consistently contains minor amounts of Ti. The size of the hematite grains is roughly proportional to that of the surrounding detrital silicates. Unlike the Cu sulfides, disseminated hematite does not form overgrowths on authigenic quartz and feldspar, and is interpreted as the metamorphic product of diagenetic and detrital Fe-Ti oxides. Hematite abundance ranges between 0.5 and 3%, much lower than the sulfide content in KLB145.

The barren gap veinlets are composed predominantly of dolomite, with lesser quartz, orthoclase, biotite, and minor specular hematite. The carbonate shows multiple stages of growth under CL, from early dark Fe-rich dolomite rhombs through successive euhedral overgrowths of varying Fe content, to a pore space filling cement of dark red luminescent dolomite (Figure 6g, h). Hematite is found within the last stage of dolomite. The veinlets have dolomite–biotite alteration haloes similar to those in KLB145 (Figure 6i, j). This paragenetic sequence is similar to that of the mineralized veins, and suggests they were coeval.

In summary, the barren gap lithologies are identical to those in the mineralized zone and preclude the possibility that the gap is lithologically controlled. There is neither any evidence to support an origin by secondary leaching of Cu sulfides. The sandstones and siltstones in the barren gap appear to have undergone the same diagenetic history, with early oxidation and weathering recorded by dust rims of Fe-Ti oxides and micas (clays), followed by later diagenetic k-feldspar and quartz overgrowths. Bedding-parallel veinlets, predominantly composed of carbonate, are present in the intersection, but are much less abundant than in the mineralized zone. There is a corresponding reduction in the amount of dolomite alteration. Specular hematite occurs mainly as disseminated grains that are texturally consistent with an origin via metamorphism of detrital and diagenetic Fe-Ti oxides.

Konkola North Orebody Margin, Drill Hole KLB83

Drill hole KLB83 was collared on the northern limb of the Kirila Bomwe Anticline, approximately 200 m east of the edge of the North ore body (Figure 1). It intersected the OS at a depth of 715.2 to 731.2 m, for a calculated true thickness of 11.7 m. Assays ranged from 0.02 to 0.09% TCu. Fleischer et al. (1976) describe the eastern margin of the North orebody as coincident with a gradual facies change from interbedded sandstones and siltstones to feldspathic arenites indistinguishable from the footwall sandstones. As in the barren gap transition, "approaching the margin of the orebody, the ore is confined to the top of the B unit and to the C unit", in other words to the carbonate-rich part of the section.

The core from KLB83 was examined briefly and three samples taken. The OS in KLB83 is underlain by 10.8 m of grey-pink, leached conglomerate (FWC) and 17.7 m of grey, medium-grained feldspathic sandstone (FWS). It is overlain by grey to pink feldspathic sandstones and minor interbedded siltstones of the HWQ. Up to 5% specular hematite occurs in both the hangingwall and footwall rocks, as angular to rounded detrital grains (probably after magnetite) and platy, often euhedral crystals (after ilmenite and diagenetic amorphous iron oxides)

In thin section, quartz overgrowths are present in the hangingwall sandstones and preserve diagenetic dust rims (Figure 6k). Hydrothermal/metamorphic biotite locally overgrows the groundmass. The footwall sandstone can be classified as a poorly sorted feldspathic greywacke, with local matrix-poor bands of feldspathic arenite. It is compositionally similar to the sandstones described from the other drill holes. Coarse-grained dolomite and biotite are intergrown and replace the detrital grains and matrix to varying degrees (Figure 6l). Under CL the dolomite shows alternate Fe-rich and Fe-poor growth zones. The presence of dolomite in the OS footwall is interesting, and may indicate migration of the altered (and mineralized?) interval - this is common elsewhere in the Copperbelt on the margins of ore bodies.

As in the barren gap, each of the subunits of the OS occurs in the KLB83 intersection, and, except for the presence of hematite, there are no apparent differences in original composition from the rocks of the mineralized intersection. The OS interval contains up to 5% mm to cm bands of dolomitic sandstone, and no significant veining. Two samples were collected, of a feldspathic greywacke at the upper contact of the OS, and of a siltstone from unit B. The feldspathic greywacke contains local quartz grains with authigenic overgrowths that preserve minute grains of hematite and rutile as "dust rims". Approximately 2% hematite also occurs as typical rounded (detrital) and platy (authigenic) grains. The siltstone contains 1 to 2% similarly textured but correspondingly smaller grains of hematite and rutile. As in KLB67, the Fe-(Ti) oxide content in the OS is much less than the Cu sulfide content in the equivalent interval. Biotite is fine-grained, and the coarse biotite associated with mineralization in KLB145 is absent.

In summary, the KLB83 intersection is similar to that of the barren gap, containing only minor amounts of carbonate alteration and veining, disseminated specular hematite after probable authigenic Fe oxides, and preserved early diagenetic dust rims on detrital grains. Additional sampling is required to more completely characterize the intersection.

Summary and Conclusions

The lithologies that host mineralization in KLB145 are indistinguishable from those in the barren holes, KLB67 and KLB83, thus there does not appear to be a lithological control on the lateral distribution of mineralization. The barren gap is not a carbonate bioherm, and in fact contains less carbonate (as alteration) than the mineralized interval. Also, the barren holes do not consistently have a different

footwall or hangingwall lithology that might control mineralization.

Diagenetic features are readily observable in the cores, and are again relatively consistent between the barren and mineralized intersections. They consist of early hematite, rutile and mica (after clay) dust rims on detrital silicate grains, which are preserved by later overgrowths of k–feldspar and quartz. No evidence was found of Cu mineralization associated with these features. Hematite present within the barren holes is identical to that in the hangingwall and footwall of the mineralized zone, but is volumetrically minor, usually less than 2%.

The Cu-Co mineralization in KLB145 is associated with hydrothermal / metamorphic ferroan dolomite, biotite and muscovite alteration and veins, in a sequence of roughly symmetric zones. The highest copper grades occur in a central, bornite-rich zone associated with abundant veins and dolomite-biotite alteration. Lower grades are found in proximal biotite-muscovite alteration where chalcopyrite dominates. Cobalt (carrolite, and possibly cobaltian chalcopyrite?) is highest where dolomite is poorly developed or absent. Coarse-grained and often irregular sulfides are most abundant in the dolomitic zone, but present throughout. Platy or bladed sulfides, likely after hematite/ilmenite, are also present throughout.

Dolomite veins and dolomite-biotite alteration also occur in the barren intersections, but lack sulfide, and are volumetrically less significant. The indication is that these holes are on the fringes of the hydrothermal system. It would be anticipated that within such a system any record of an earlier mineralization event would be destroyed, and the mineralized zone in KLB145 in fact lacks such a record. However, it might also be expected that any earlier event would be preserved on the margins of the hydrothermal system, and this is not the case. It is therefore difficult to argue for there being two superimposed mineralizing events at Konkola.

Future work will include completing a sulfur isotopic study on the mineralization to determine whether any variation exists amongst the texturally different sulfides, and SEM/EDS study of the biotite to determine whether metamorphic and hydrothermal phases can be distinguished.

References

Fleischer, V.D., Garlick, W.G., and Haldane, R., 1976, Geology of the Zambian Copperbelt, *in* Wolf, K.H., ed., Handbook of Strata-bound and Stratiform Ore Deposits, Volume 6: Elsevier, Amsterdam, p. 223-352.

Sweeney, M.A., and Binda, P.L., 1989, The role of diagenesis in the formation of the Konkola Cu-Co orebody of the Zambian Copperbelt, *in* Boyle, R.W. et al., eds, Sediment-hosted Stratiform Copper Deposits, Geol. Assoc. Canada Sp. P. 36, p. 499-518.